AD-A173 550 TELECONNECTIONS AND SEA ICE VARIABILITY IN THE GREENLAND SEA(U) NAVAL POSTGRADUATE SCHOOL MONTEREY CA W A WILSON JUN 86 1/1

UNCLASSIFIED F/G 8/12 NL

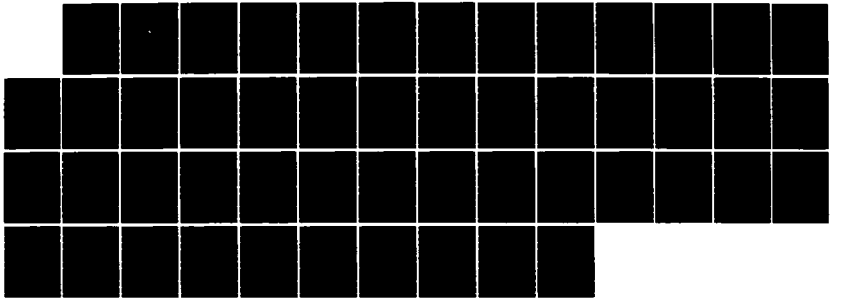

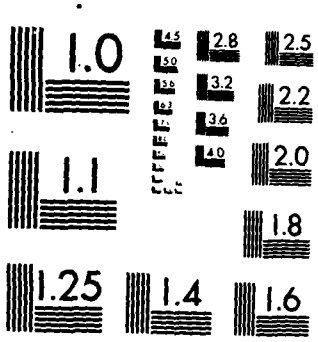

(2)

NAVAL POSTGRADUATE SCHOOL
Monterey, California

THESIS

Teleconenctions and Sea Ice Variability
in the Greenland Sea

by

Ward A. Wilson III

June 1986

Thesis Advisor: R. W. Garwood

UNCLASSIFIED
SECURITY CLASSIFICATION OF THIS PAGE

AD-A173 550

REPORT DOCUMENTATION PAGE

1a REPORT SECURITY CLASSIFICATION UNCLASSIFIED	1b. RESTRICTIVE MARKINGS
2a SECURITY CLASSIFICATION AUTHORITY	3 DISTRIBUTION/AVAILABILITY OF REPORT DISTRIBUTION STATEMENT A Approved for public release; Distribution Unlimited
2b DECLASSIFICATION / DOWNGRADING SCHEDULE	
4 PERFORMING ORGANIZATION REPORT NUMBER(S)	5 MONITORING ORGANIZATION REPORT NUMBER(S)
6a. NAME OF PERFORMING ORGANIZATION Naval Postgraduate School 6b. OFFICE SYMBOL (If applicable) 68	7a. NAME OF MONITORING ORGANIZATION Naval Postgraduate School
6c ADDRESS (City, State, and ZIP Code) Monterey, California 93943-5000	7b. ADDRESS (City, State, and ZIP Code) Monterey, California 93943-5000
8a NAME OF FUNDING / SPONSORING ORGANIZATION 8b. OFFICE SYMBOL (If applicable)	9. PROCUREMENT INSTRUMENT IDENTIFICATION NUMBER
8c ADDRESS (City, State, and ZIP Code)	10 SOURCE OF FUNDING NUMBERS PROGRAM ELEMENT NO / PROJECT NO / TASK NO / WORK UNIT ACCESSION NO

11 TITLE (Include Security Classification)

TELECONNECTIONS AND SEA ICE VARIABILITY IN THE GREENLAND SEA

12 PERSONAL AUTHOR(S)
Ward A. Wilson

13a TYPE OF REPORT	13b TIME COVERED	14 DATE OF REPORT (Year, Month, Day)	15 PAGE COUNT
Master's Thesis	FROM _____ TO _____	June 1986	50

16 SUPPLEMENTARY NOTATION

17 COSATI CODES			18 SUBJECT TERMS (Continue on reverse if necessary and identify by block number)
FIELD	GROUP	SUB-GROUP	Sea ice, El Nino, air sea interactions

19 ABSTRACT (Continue on reverse if necessary and identify by block number)

The hypothesis that the sea ice variability in the Greenland Sea is related to atmospheric teleconnections is tested. The teleconnections included in this test are the Southern Oscillation Index (SOI) and the North Atlantic Oscillation Index (NAO). Anomalous monthly time series for the sea ice extent, SOI, and the NAO are examined for the 25-year period of 1953-1977. The results show that the sea ice anomaly is negatively correlated with the SOI anomaly when the sea ice lags the SOI 24 to 29 months. Cross-correlations of the data sets by season failed to reveal any significant seasonal dependence.

20 DISTRIBUTION / AVAILABILITY OF ABSTRACT	21 ABSTRACT SECURITY CLASSIFICATION
☒ UNCLASSIFIED/UNLIMITED ☐ SAME AS RPT ☐ DTIC USERS	UNCLASSIFIED
22a NAME OF RESPONSIBLE INDIVIDUAL R. W. Garwood	22b TELEPHONE (Include Area Code) 408-646-3206 / 22c OFFICE SYMBOL 68Gd

DD FORM 1473, 84 MAR 83 APR edition may be used until exhausted
All other editions are obsolete

SECURITY CLASSIFICATION OF THIS PAGE
UNCLASSIFIED

Approved for public release; distribution is unlimited.

Teleconnections and Sea Ice Variability in the Greenland Sea

by

Ward A. Wilson III
Lieutenant, United States Navy
B.S., High Point College, 1980

Submitted in partial fulfillment of the
requirements for the degree of

MASTER OF SCIENCE IN METEOROLOGY AND OCEANOGRAPHY

from the

NAVAL POSTGRADUATE SCHOOL
June 1986

Author: _____
Ward A. Wilson III

Approved by: _____
R.W. Garwood, Thesis Advisor

_____
H.J. Niebauer, Co-Advisor

_____
C.N.K. Mooers, Chairman,
Department of Oceanography

_____
John M. Dyer,
Dean of Science and Engineering

ABSTRACT

The hypothesis that the sea ice variability in the Greenland Sea is related to atmospheric teleconnections is tested. The teleconnections included in this test are the Southern Oscillation Index (SOI) and the North Atlantic Oscillation Index (NAO). Anomalous monthly time series for the sea ice extent, SOI, and the NAO are examined for the 25-year period of 1953-1977. The results show that the sea ice anomaly is negatively correlated with the SOI anomaly when the sea ice lags the SOI 24 to 29 months. Also, the sea ice anomaly is found to be negatively correlated with the NAO anomaly when the sea ice lags the NAO 0 to 2 months. Cross-correlations of the data sets by season failed to reveal any significant seasonal dependence.

TABLE OF CONTENTS

LIST OF FIGURES

ACKNOWLEDGEMENTS

The author thanks Professor Roland W. Garwood for guidance throughout the thesis project. Thanks also go to Professor H.J. Niebauer, Arlene Bird, and D.R. McLain. A special thanks to my wife Ann, for typing much of the thesis.

I. INTRODUCTION

A. PURPOSE AND MOTIVATION

The purpose of this study is to examine and test the hypothesis that the multiyear sea ice variability in the East Greenland Current is related to the El Nino/Southern Oscillation phenomenon and/or the North Atlantic Oscillation via atmospheric teleconnections. "Teleconnection" is defined here, after Wallace and Gutzler (1981), as significant simultaneous correlations between temporal fluctuations in oceanic and atmospheric parameters at widely separated points on the earth.

The ability to forecast or predict long term sea ice anomalies in the waters off the east coast of Greenland and in the Denmark Straight is of vital interest to civilian concerns and the U.S. Navy alike.

The shipping, fishing, and oil industries are concerned with sea ice coverage. Surface shipping industries of maritime nations use optimal track routing services to avoid areas of sea ice. Fishing fleets may be denied choice fishing grounds due to heavy sea ice. Oil drilling platforms must be built to withstand the forces of drifting sea ice.

While the U.S. Navy is also concerned with the safety of shipping around or through sea ice covered areas, there are tactical and strategic applications associated with the extent and movement of sea ice in the East Greenland Current.

One important aspect of Naval operations is in the area of submarine detection and tracking in the vicinity of the

sea ice edge. Soviet ballistic missile submarines do not have to travel far from their Northern Fleet ports to be in the waters off the East Greenland coast. Urick (1983) notes that at the edge of an ice sheet, a strong source of underwater acoustic noise is the water slapping against the ice and that this noise can be 12 decibels higher in the 100 to 1000 Hz range than in the open sea. This implies that a submarine could use to a tactical advantage the area where the sea ice edge is located. The antisubmarine warfare capability would be limited to underwater methods and tactics as surface ships and aircraft would be ineffective due to the physical barrier of the sea ice. The implication here is that antisubmarine warfare in the polar and subpolar seas is likely to be dependent upon variability in the ice. Knowledge of and prediction of this variability is therefore of interest to the Navy. Figure 1.1 shows the mean maximum and minimum sea ice extent for the Greenland Sea. During very heavy ice years the western side of Iceland can be ice bound.

B. METHOD AND BACKGROUND

The method for testing the hypothesis consists primarily of cross correlation analysis. Twenty-five year time series of the Southern Oscillation Index (SOI) and the North Atlantic Oscillation (NAO) are examined, and their respective anomalies are correlated with the anomalous areal extent of sea ice off the east coast of Greenland. Figure 1.2 shows the area where sea ice extent is considered. The area includes the entire length of the East Greenland Current and the area around Iceland. This total area is 790,200 nautical miles. Cross correlation coefficients will be calculated for the departure from the monthly mean fields for the years 1953 to 1977. The midlatitude westerlies must extend into the equatorial troposphere over the region of a

heat source; such as, the warm sea surface temperature associated with an ENSO event, for a teleconnection to extratropical latitudes to occur (Horel and Wallace,1981). Hence the Northern Hemisphere winter months of December, January, February (DJF) are of possible special interest, and they will be examined for cross correlations among the data sets in the manner of Horel and Wallace (1981). The correlations will be examined for the other seasons in a similar manner, systematically testing for seasonal dependence.

1. Sea Ice Formation, Processes and Climatology

The air-sea-ice interactions in the Arctic Sea are complex and important to the oceanography and meteorology of the Arctic region and their effects extend to the peripheral northern seas such as the Bering and Greenland Seas. Coachman and Aagard (1974) discussed some of the unique features of air-sea-ice interactions in polar regions as follows:

1. The water temperature adjacent to ice near the surface is quite close to freezing, and this temperature depends on the salinity.
2. When sea water freezes, salt is expelled as brine at a rate depending on the age of the ice.
3. The sea water under the ice is more saline as a result of this freezing. The increased salinity near the surface can reduce hydrostatic stability and possibly lead to vertical convection and mixing.
4. The transfer of momentum from the atmosphere to the ocean must pass through the sea-ice interface.

Walsh (1983) describes some other properties of sea ice such as the increase in surface albedo with sea ice cover and the low thermal conductivity of sea ice, which tends to insulate the ocean from the atmosphere.

The actual mechanism of air-sea interactions which produces fluctuations in the latitudinal and longitudinal polar sea ice extent is not readily apparent. Walsh and Johnson (1979) have shown that the equatorward extent of

polar sea ice can vary by up to five degrees of latitude in the peripheral seas of the Arctic. The areas with the largest standard deviation in the departure from the monthly means of sea ice extent are the eastern Bering Sea and the Greenland Sea, including the Denmark Strait. Anomalies in the longitudinal extent of sea ice exist in the Arctic where the anomaly of the sea ice coverage in the Bering Sea may be out of phase with the anomaly in the waters off the East Greenland Coast. Smirnov (1980) proposed that the anomalies of sea ice coverage in the eastern and western Arctic are 180 degrees out of phase. Walsh and Sater (1981) find a correlation of -0.38 between sea ice coverage for the Bering Sea and the coverage for the waters off the east coast of Greenland. However, the 95% significance level in this case was 0.40, so the negative correlation is marginal.

The East Greenland Current (EGC) is a major outlet for Artic pack ice and drift ice with up to one third of the Arctic pack ice being carried away each year (Pickard and Emery, 1982). The EGC is a southward flowing current and part of the general cyclonic circulation of the Greenland Sea. The speed of the EGC has been estimated at 0.3 to 0.8 kts by Sater,Ronhovde and Van Allen (1971). In addition to sea ice, the EGC carries Arctic water of low salinity down the entire length of the east coast of Greenland and around Kap Farvel.

2. El Nino/Southern Oscillation

El-Nino is the name applied to the phenomenon where anomalously warm water appears over a widespread area off the northwest coast of South America. El Nino events have been studied extensively by Walker and Bliss (1932), Bjerknes (1961, 1969), Wyrkti (1975, 1982), and others. Walker and Bliss (1932) originated the term "Southern Oscillation" in their discussion of the east-west transfer

of air mass in the equatorial Pacific Ocean. Bjerknes (1961) suggested that very weak trade winds along the west coast of South America would lead to an end of coastal upwelling and allow warm equatorial water to reach the coast. Wyrkti (1975) combined many of the separate ideas to propose a theory for El Nino that has been generally well accepted. He reasoned that prior to an El Nino event, the southeast trades are excessively strong and intensify the subtropical gyre of the South Pacific. This would then lead to an increase in the east-west slope of the sea surface. The accumulated warm water in the west would flow eastward when the wind stress slackened. The accumulation of warm water then depresses the thermocline off the west coast of South America and inhibits the upwelling of cold nutrient-rich water. This can then result in severe stress on the biological ecosystem, and a significant reduction in the potential fishery resource.

The Southern Oscillation Index (SOI) is the difference in sea level pressure anomalies between Tahiti and Darwin, Australia. Darwin lies in the Indonesian-Australian low, and Tahiti lies in the Southeast Pacific subtropical high region. Therefore the magnitude of the SOI should indicate the strength of the trades. El Nino and the SOI are thought to be closely interrelated, and the acronym ENSO (El Nino-Southern Oscillation) has been applied to the combined phenomena.

Rasmusson and Carpenter (1982) describe the typical stages of an ENSO event. However, the most recent, and one of the strongest, ENSO events, that of 1982 to 1983, was not typical of prior events in that the appearance of warm sea surface temperatures first occurred in the central rather than in the eastern Pacific. Also, this event lasted longer than previous ones. The data sets in this study cover the

period from 1953 to 1977, so the important 1982 to 1983 ENSO event will not be analyzed. During the time frame of this study, there have been at least five ENSO events of note as defined by Quinn, Zopf, Short, and Kuo Yang (1978). These years are 1953, 1957, 1965, 1972, and 1976.

ENSO events appear to have an influence on some of the meteorological and oceanographic parameters in the extra-tropical latitudes through the enhancement of the Hadley circulation in the Pacific area. A deepening and southward displacement of the Aleutian low during the Northern Hemisphere winter has been related to ENSO (Bjerknes, 1966; Horel and Wallace, 1981). Niebauer (1984) indicates a significant positive correlation between the SOI and air temperature in the vicinity of the Pribilof Islands. The SOI and other atmospheric data fields such as the Northern Hemisphere geopotential height anomalies have been shown to be statistically significant and dynamically consistent (Horel and Wallace, 1981).

3. North Atlantic Oscillation

The North Atlantic Oscillation (NAO) is a north-south oscillation while the SOI is oriented east-west. The NAO is defined as the difference in normalized sea level pressure between a wide band of high pressure at 40N and a low pressure center around 65N in the North Atlantic. Walker and Bliss (1932) and Wallace and Gutzler (1981) note the following characteristics for the NAO:

1. A negative correlation exists in the mean surface temperatures between the Greenland/Labrador region and Northwestern Europe.
2. A negative correlation exists in the sea level pressure between the area of the Icelandic low around 65 degrees north and a large east-west zone of high pressure near 40 degrees north.

The negative correlation in winter temperatures is supported by van Loon and Rogers (1978), and the negative

correlation in sea level pressure is also shown by Kutzbach (1970). The dynamics of the NAO as outlined by Wallace and Gutzler (1981) are that a deep Icelandic low produces cold air advection over Greenland and warm air advection over Europe, resulting in the temperature correlation observed.

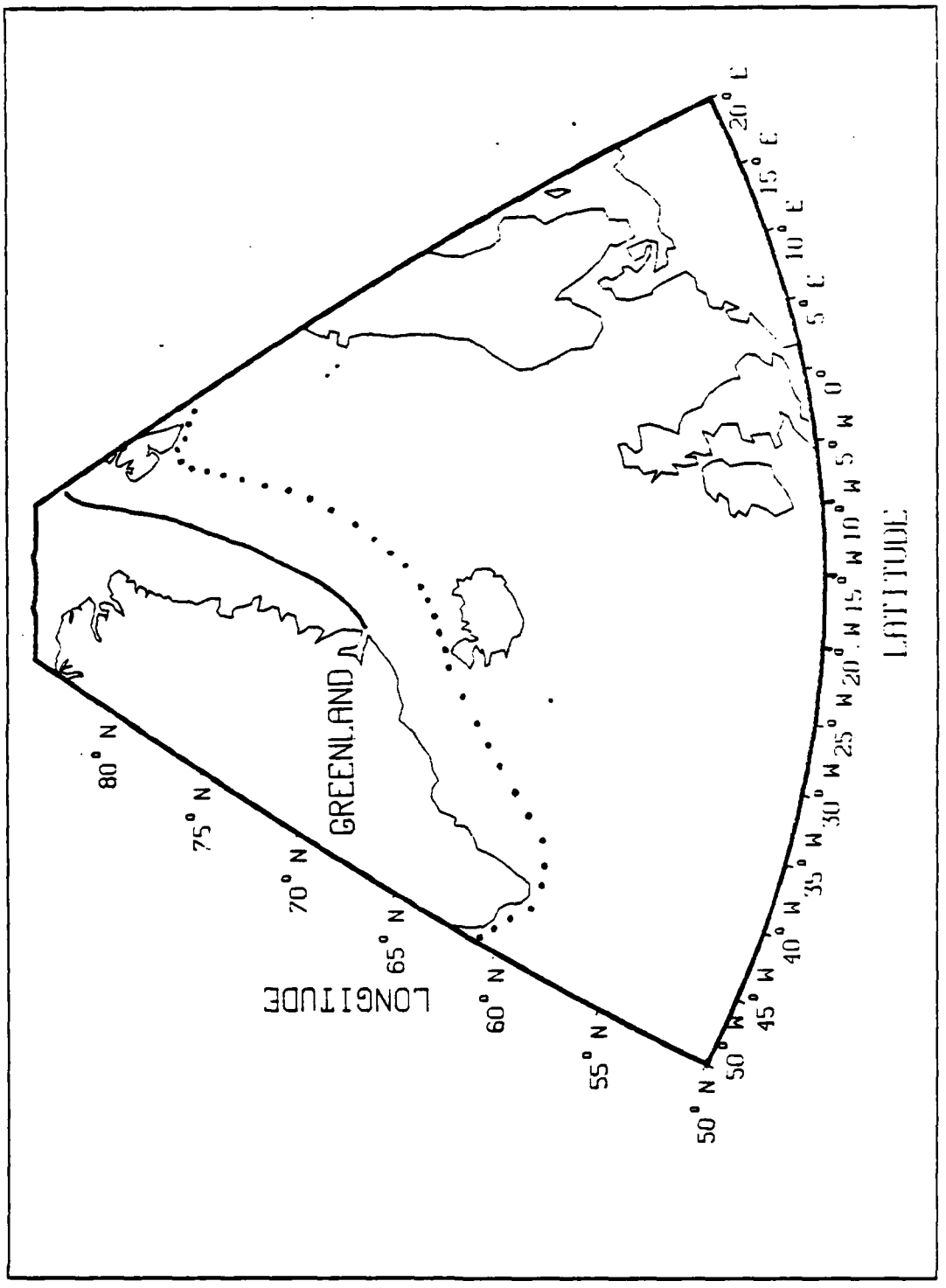

Figure 1.1 Mean Maximum (___) and Minimum (...) Ice Extent.

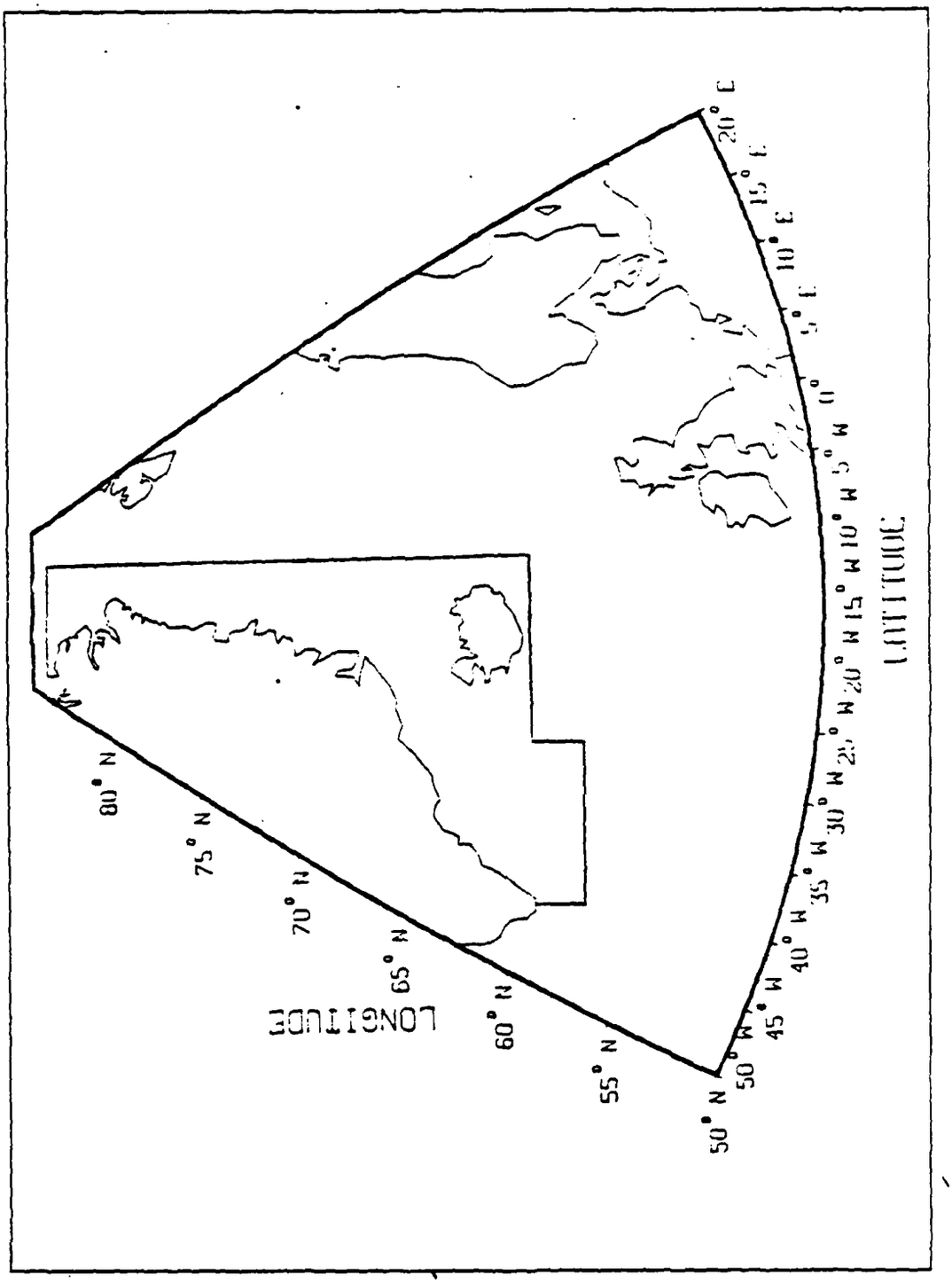

Figure 1.2 Area of Interest.

II. DATA, MEAN FIELDS, AND ANOMALIES

A. SEA ICE

Prior to the Second World War, observations and measurements of sea ice areal extent were neither systematic nor complete. Since then, the regular use of aircraft reconnaissance, drifting buoys, ship reports, and satellite observations has increased the number and accuracy of sea ice coverage reports. In this and the following two subsections the data sets are defined and time series plots of the mean and departures from the mean are discussed.

The sea ice coverage data set considered in this study was obtained from J.E. Walsh and is a subset of the Arctic sea ice coverage observations from 1953 to 1977 amassed by Walsh and Johnson (1979). The original sea ice data were obtained from monthly ice concentration grids. The grids were compiled by Walsh and Johnson (1979) from various reporting agencies in the United States, Canada, Great Britain, Denmark, Norway, and Iceland. Each grid is 60 nautical miles on a side, and sea ice coverage is represented in tenths. A sea ice coverage report of 10/10 would represent a grid point completely covered by sea ice. The sea ice concentration data only includes the sea ice areal extent. Neither ice type nor ice thickness information are available. Hence, 3 m thick ice is treated the same as 3 cm thick ice. A separate array containing the ocean area corresponding to each ice grid point is used for computing the ice covered ocean area. The mean extent of sea ice is the sum (over all grid points in the region) of the product of the grid point concentration and the corresponding ocean area. (Walsh and Johnson, 1979). A time series plot of the mean monthly percentage of sea ice cover is shown in Figure

2.1. The strong periodic signal indicates more ice cover in the winter months than non-winter months. There also appears to be a long term trend in the percent of ice cover showing an increase in the mean ice coverage in the late 1960's. The 25-year mean has been removed so the values are plotted relative to zero. The values of sea ice cover above zero indicate coverage in excess of the mean and negative values show coverage less than the mean. The departures from the mean for each data set (sea ice, SOI, NAO) was calculated by first finding the 25-year monthly mean for each month (mean for all January's, February's, etc.) and then subtracting the 25- year monthly mean from the respective months. Figure 2.2 shows the departures from the mean ice cover or anomalous ice cover for 1953 to 1977. A twelve-month running mean is also plotted. Both signals show an increase in ice cover from 1958 to 1963 and 1966 to 1977 as did the unsmoothed data. A general decrease in the sea ice extent from 1970 to 1977 is observed. Walsh and Sater (1982) note that the Bering Sea ice decreased in the late 1960's and increased in the early 1970's. The sea ice values used in the correlation analysis are the departure from the 25 year monthly mean fields.

B. ENSO

The difference in the normalized sea level pressure between Tahiti in the South Pacific and Darwin, Australia, is defined as the Southern Oscillation Index (SOI) and equals Tahiti sea level pressure minus Darwin sea level pressure. The monthly mean sea level pressure data were acquired from Trenberth (1984). Figure 2.3 shows the 25-year time series plot of monthly mean SOI values along with a twelve-month running mean. The plot is relative to zero with positive values indicating a relatively greater atmospheric pressure difference between Tahiti and Darwin

than the SOI is negative. The range of monthly mean values for the SOI is from 8 to -10 mb. Figure 2.4 shows the SOI departures from the mean or anomalous time series with a twelve-month running mean. The range of the SOI anomaly values is from 7 to -8 mb. The positive anomalies indicate the positive phase of the SOI, and negative anomalies show the negative phase of the SOI. The positive phase of the SOI correspondes to the time period before an ENSO event, and the change to a negative anomaly signals the oncoming ENSO (Wyrkti, 1982). The ENSO events that have taken place during the period of the data set can be seen where the SOI anomaly is most negative. The negative phase of the SOI of signalling an ENSO event is preceded by a positive anomaly in the SOI in each of the ENSO event years of 1957,1965,1972,and 1976 as seen in the 12 month running mean in Figure 2.4.

C. NAO

The NAO data are the difference in normalized sea level pressure between 45N, 30W and 60N,30W where the pressure at 60N (a climatological low) is subtracted from the pressure at 45N (a climatological high). The data were acquired from the Fleet Numerical Oceanography Center, Monterey, California via D.R. McLain of the NOAA National Marine Fisheries Service. A maximum in the differences between the respective sea level pressures should be indicative of a strong Icelandic Low. This is one of the characteristics of the NAO described by Wallace and Gutzler (1981) and discussed in the previous chapter. Figure 2.5 shows the NAO monthly mean time series and twelve-month running mean which are relative to zero, where positive values indicate a relatively larger pressure difference between the two areas of interest and correspondingly deeper Icelandic low. The range of values for the NAO time series

is from 21 to -27 mb. The NAO time series is a higher-frequency, shorter-period signal than the SOI time series.

Figure 2.6 shows the 25-year monthly mean anomaly of the NAO with a twelve-month running mean. The NAO anomalies show a greater range in value than the SOI anomalies. The NAO anomaly values range from 16 to -28 mb. In the next chapter, cross-correlations will be calculated between the NAO anomaly data set and the sea ice anomaly data set by month and by season, as well as with the SOI anomaly data set by month.

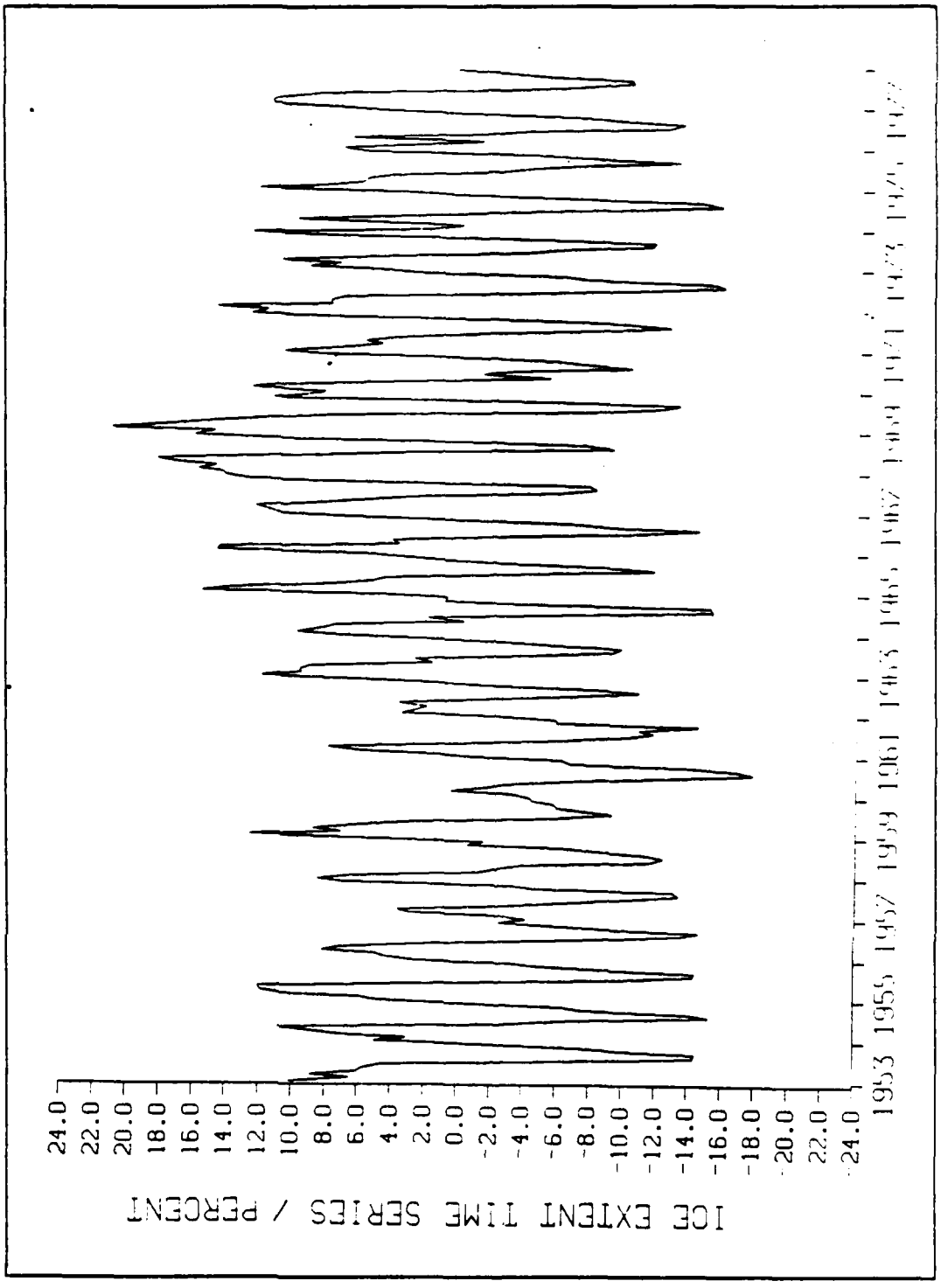

Figure 2.1 Monthly Mean Percent Sea Ice Cover.

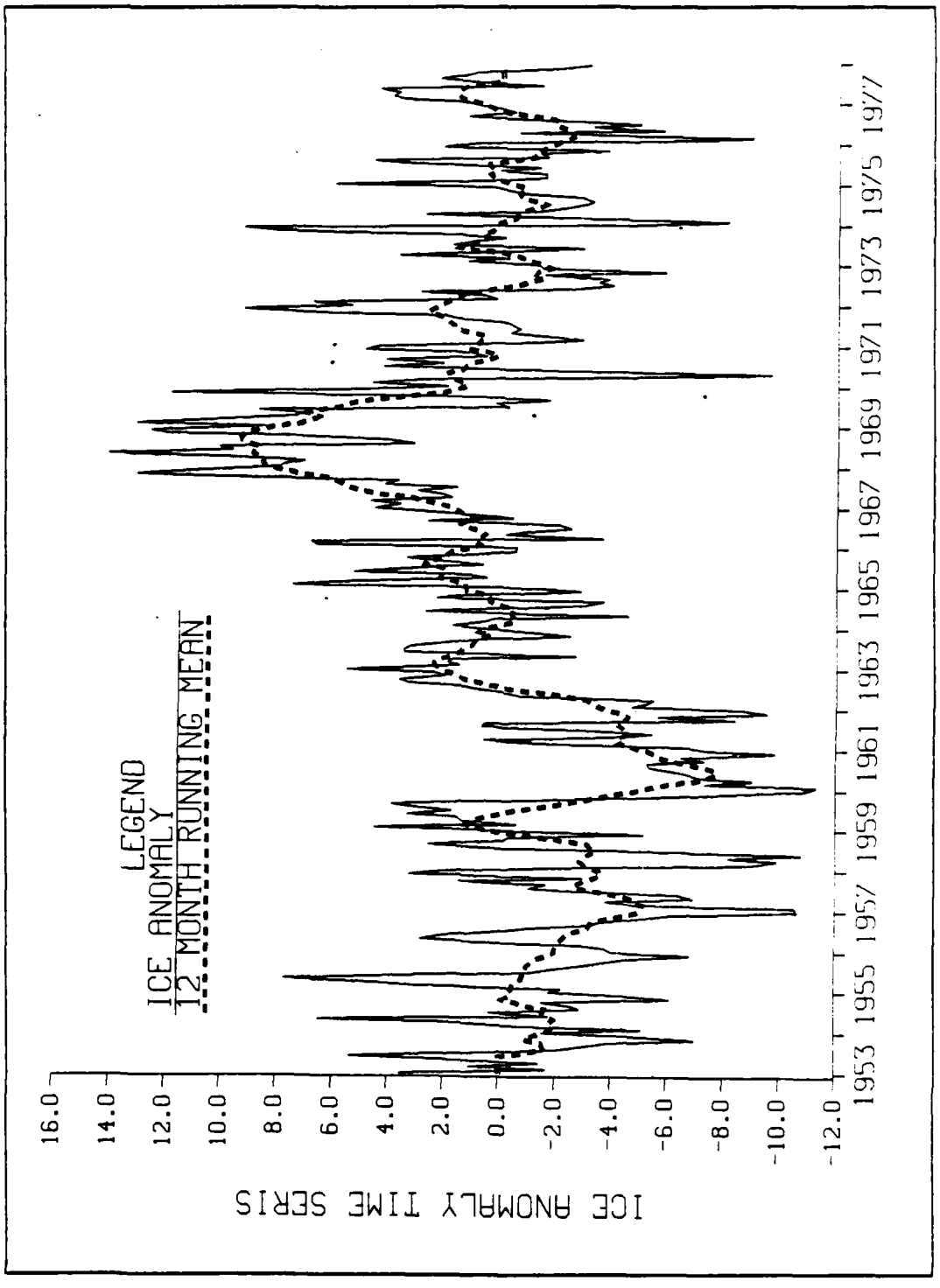

Figure 2.2 Percent Sea Ice Cover Anomaly.

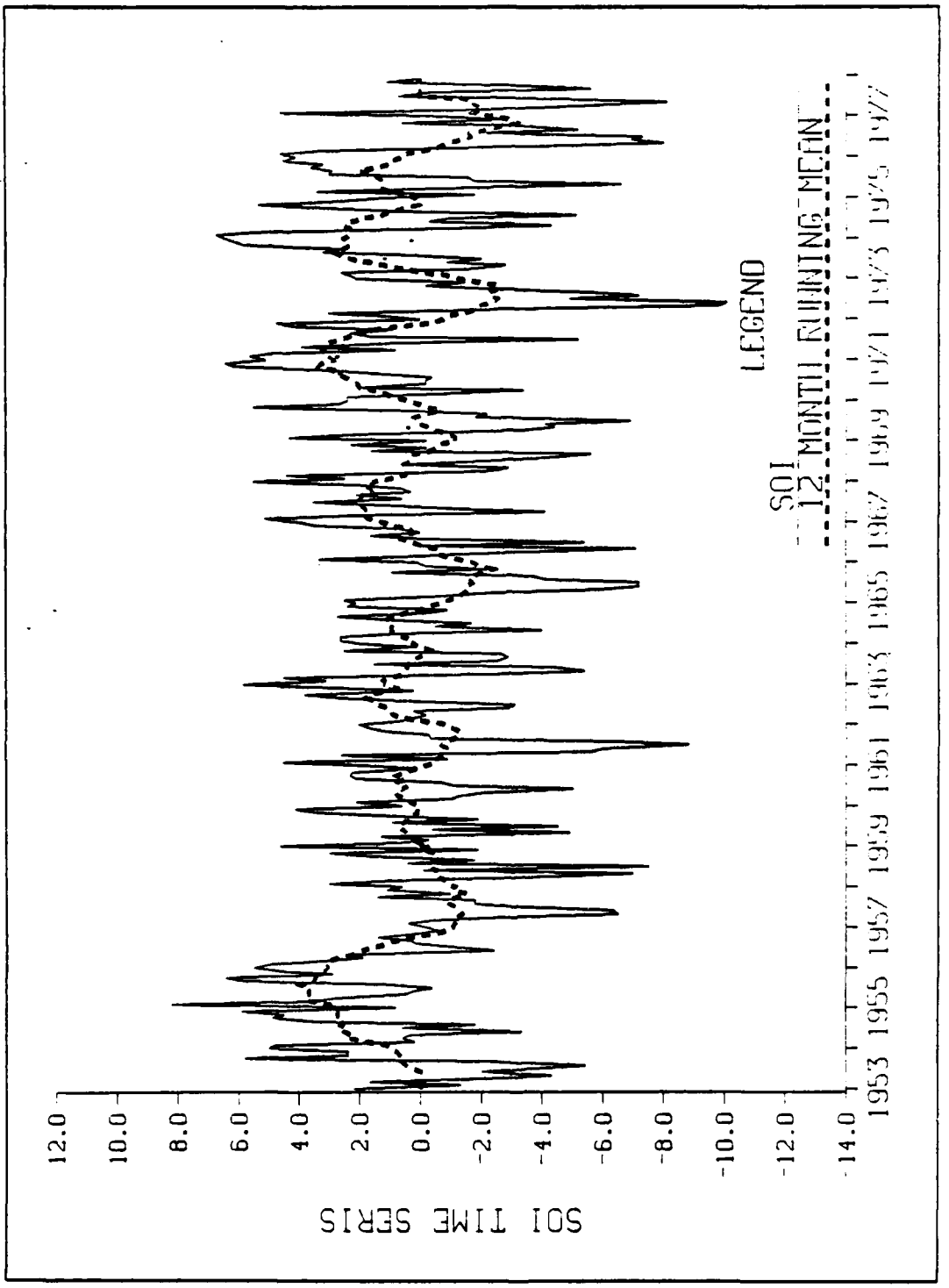

Figure 2.3 Monthly Mean SOI.

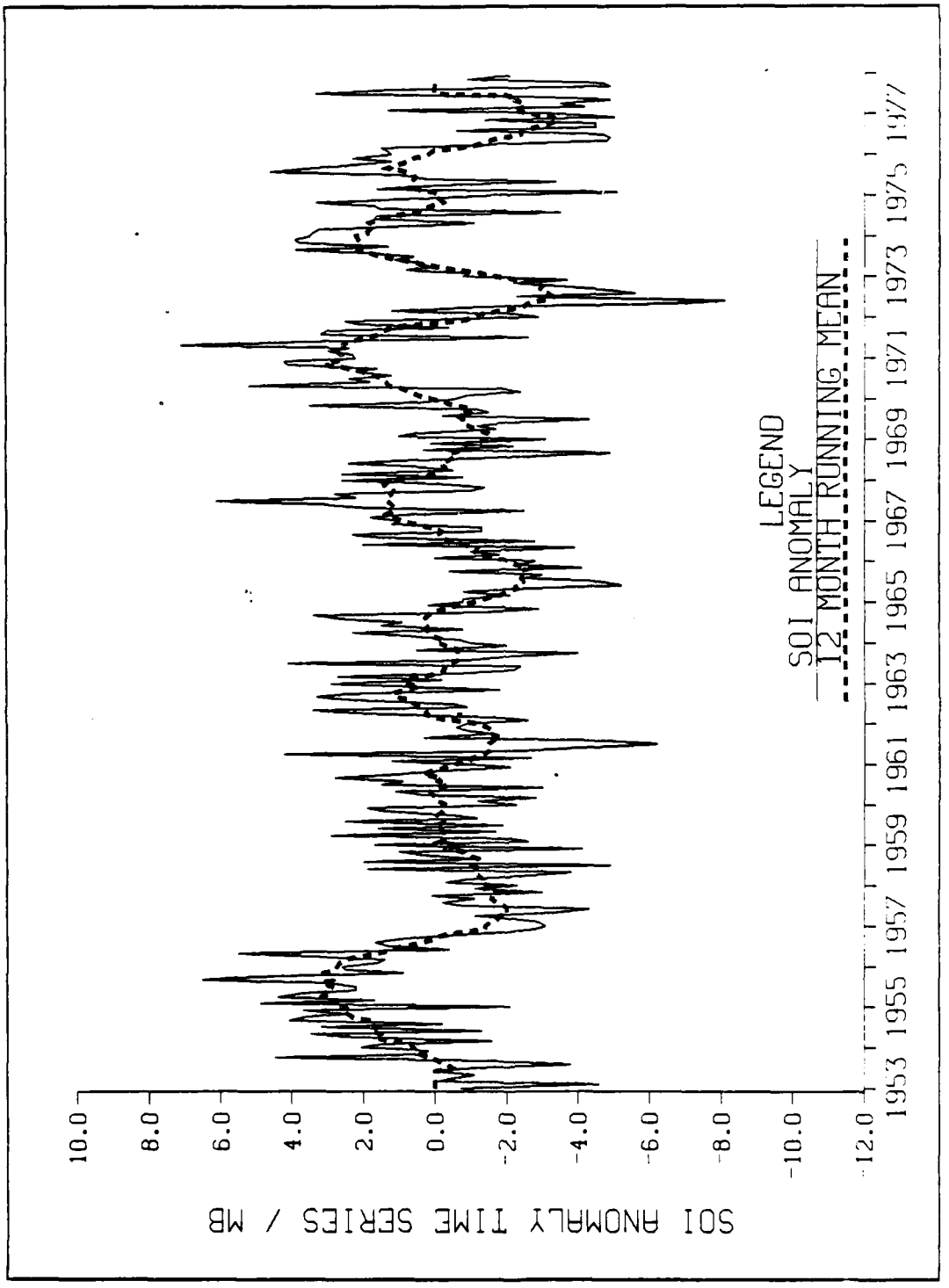

Figure 2.4 SOI Anomaly.

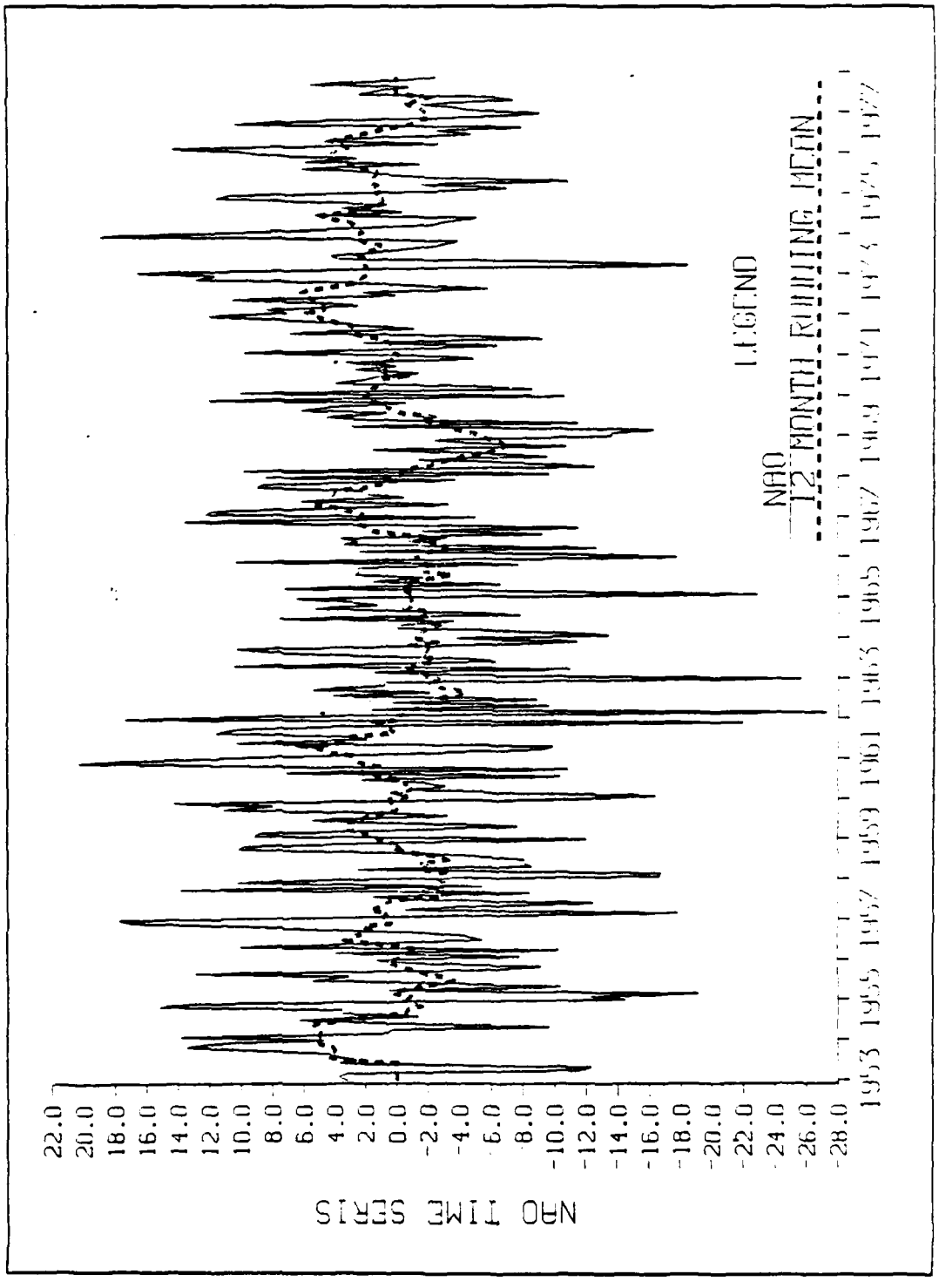

Figure 2.5 Monthly Mean NAO.

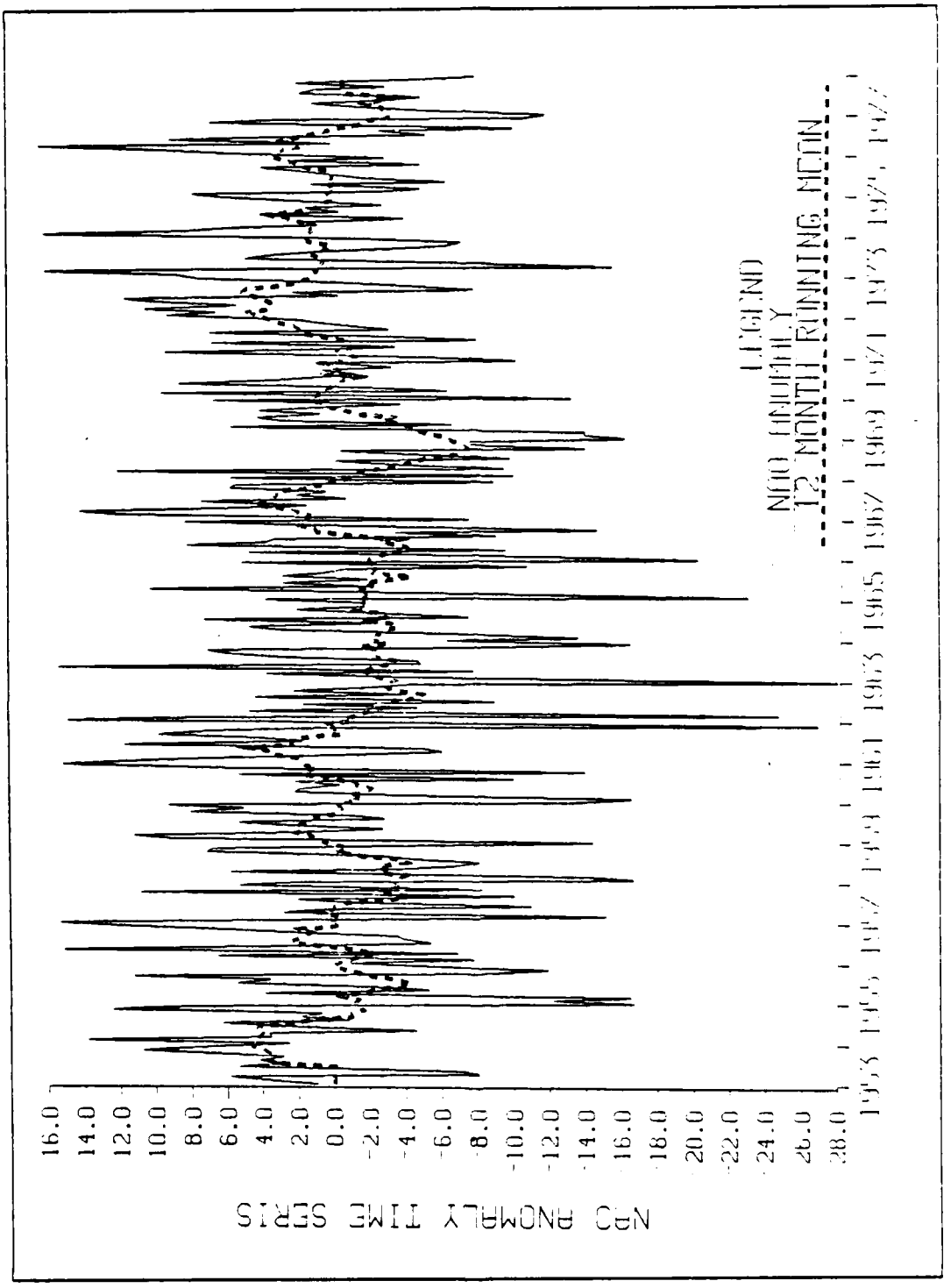

Figure 2.6 NAO Anomaly.

III. ANALYSIS AND CROSS-CORRELATIONS

A. SOI AND ICE ANOMALY CROSS-CORRELATIONS

Figure 3.1 is a plot of the SOI and sea ice anomaly's cross- correlation function (CCF). If the absolute value of the CCF value should exceed the absolute value of the 95% significance level, then the correlation is said to be statistically significant. As can be seen in Figure 3.1, the absolute value of the SOI and sea ice CCF exceeds the 95% significance level (0.115). Hence, the SOI and sea ice anomalies are significantly negatively correlated between 24 and 29 months lag time. The extreme CCF value is -0.165 at a lag of 26 months. This negative correlation shows that 24 to 29 months after the SOI is in a negative phase there is an increase in the sea ice coverage in the Greenland Sea. There is also significant positive correlation when the ice leads the SOI at 18 months and 22.5 to 25 months. Niebauer (1984, 1986) correlated ENSO events with atmospheric and oceanic parameters for the Bering Sea and found significant positive correlation of 0.47 for the SOI and air temperature anomalies at the Pribolof Islands. A positive correlation of 0.26 was shown for the SOI and sea ice in the Bering Sea with the correlation persisting up to two years where sea ice lagged the SOI. A possible explanation of the negative correlation of SOI and sea ice in the Greenland Sea may be related to the negative correlation between the Bering Sea ice and the Greenland Sea ice as discussed in Chapter 1. Smirnov (1980) reports a negative correlation in the sea ice extent for the eastern and western areas of the Arctic.

An examination of the cross-correlations of the SOI and ice anomalies by season may provide support for the correlation evident in Figure 3.1. The time series were

divided into the component seasons with December, January, and February (DJF) representing the winter season. The Northern Hemisphere winter is the period that Horel and Wallace (1981) suggest is most influenced by the wide spread warm sea surface temperature brought on by El Nino in the equatorial Pacific Ocean . Horel and Wallace (1981) also discuss theoretical models which show a Rossby wave train emanating from a heat source with positive and negative geopotential height anomalies extending from the North Pacific to the Southeast United States. The heat source here is the warm sea surface temperature anomaly in the equatorial Pacific during the Northern Hemisphere's winter season.

In addition to the winter (DJF) season, the other seasons are examined similarly. Each season is averaged for the 25-year data set giving a data set which consists of but 25 values. With a record length of only 25 points, a cross-correlation lag of 2 to 2.5 years is the longest lag time that can be examined statistically. This is due to the maximum shifting of the data sets being limited to 10% of the record length. Both sides of the correlation function are shown.

Figure 3.2 shows the CCF of the SOI and ice anomaly for DJF. This plot shows no significant correlation at any lag or lead time. Figure 3.3 shows the CCF for the SOI and ice anomaly for March, April, and May (MAM). The extreme CCF value is -0.33 at a lag of 2.3 years; however, the correlation is not significant. There is no significant correlation when the ice leads the SOI. Figure 3.4 shows the CCF for the SOI and ice anomalies for June, July , and August (JJA). The largest CCF value is 0.32 at 0 years lag. Again, the correlation is not significant for any lag or lead time. Figure 3.5 shows the CCF for the SOI and the ice

anomalies for September, October, and November (SON). The largest CCF value is -0.36 at 1.2 years lag, and, as for the previous three seasons, it is not found to be significant. There is no significant correlation when the ice leads the SOI.

B. NOA AND ICE CROSS-CORRELATION

The following section concerns the CCF for the NAO and ice extent anomalies in the Greenland Sea. Figure 3.6 is a plot of the NAO and .sea ice anomaly's CCF by month. It shows the NAO and sea ice anomalies to be negatively correlated from 0 to 2 months lag. The extreme CCF value is -0.152 at a lag of one month. After two months there is no significant correlation. This indicates that when the NAO is in a positive phase then there is a decrease in sea ice extent. The Icelandic low is a semi-permanent feature having a climatological mean position of 60N, 30W. The flow to the north of the low is westward and is perpendicular to the East Greenland Current. The effect of the westward wind flow is to retard the southward advection of sea ice by the East Greenland Current. Ketchum and Wittmann (1971) show that ice drift in the EGC can be retarded when the geostrophic air flow is nearly perpendicular to the EGC. The time scale of 0 to 2 months lag of ice behind the NAO appears reasonable. There is no significant correlation when ice leads the NAO.

As with the CCF for the SOI and sea ice, the CCF for the NAO and sea ice will be examined by season. Figure 3.8 shows the CCF for the NAO and ice anomalies for DJF. The extreme CCF value in Figure 3.8 is -0.46 at a lag of 3.3 years. When the ice leads the NAO there is positive correlation beyond three years. The length of record is limited to 25 points, so any value of the CCF beyond 2.5 years is suspect and cannot be regarded with confidence.

Figure 3.9 shows the CCF value for the NAO and ice anomalies for MAM. While all of the CCF values are positive in this plot with a maximum of 0.3, when the lags the NAO, none of the correlations are significant. Again, there is no significant correlation when ice leads the NAO. Figure 3.10 shows the CCF value for the NAO and ice anomalies for JJA. All the CCF values out to a lag of 2.5 years are positive and minimal with no CCF value exceeding 0.19. This is the summer period where the ice cover is close to a minimum in extent and the NAO is weak. The CCF, when ice leads the NAO, shows an extreme value of 0.38 at two years. This correlation is not significant. Figure 3.11 is the CCF plot for NAO and ice anomalies for SON. There is a significant negative correlation at a lag of 1.9 to 2.5 years. This relatively extreme correlation of -0.42 is interesting since the NOA is a higher- frequency, shorter-period signal than the SOI. This indicates that two years following a phase change in the NAO there is an opposite change in the sea ice extent. This two year lag in the signal is not supported by Figure 3.1. The fall season is a strong transition period for both the sea ice and the Icelandic low, may cause this result.

C. SOI AND NAO ANOMALY CROSS-CORRELATIONS

The anomalies for the SOI and the NAO were cross-correlated to find if there is some interaction between the ENSO and the NAO. Figure 3.11 shows the CCF for the SOI and NAO anomalies. There is a marginal positive correlation of 0.41 between SOI and the NAO at the two month lag point, and none thereafter. This correlation would indicate that a negative phase in the SOI is followed 2 months later by a negative phase in the NAO, but it does not persist for any length of time. As mentioned in the previous section, the NAO is a higher frequency signal than

the SOI, and this particular correlation is difficult to explain using these data sets. The correlations thus far presented, are in most cases, not definitive.

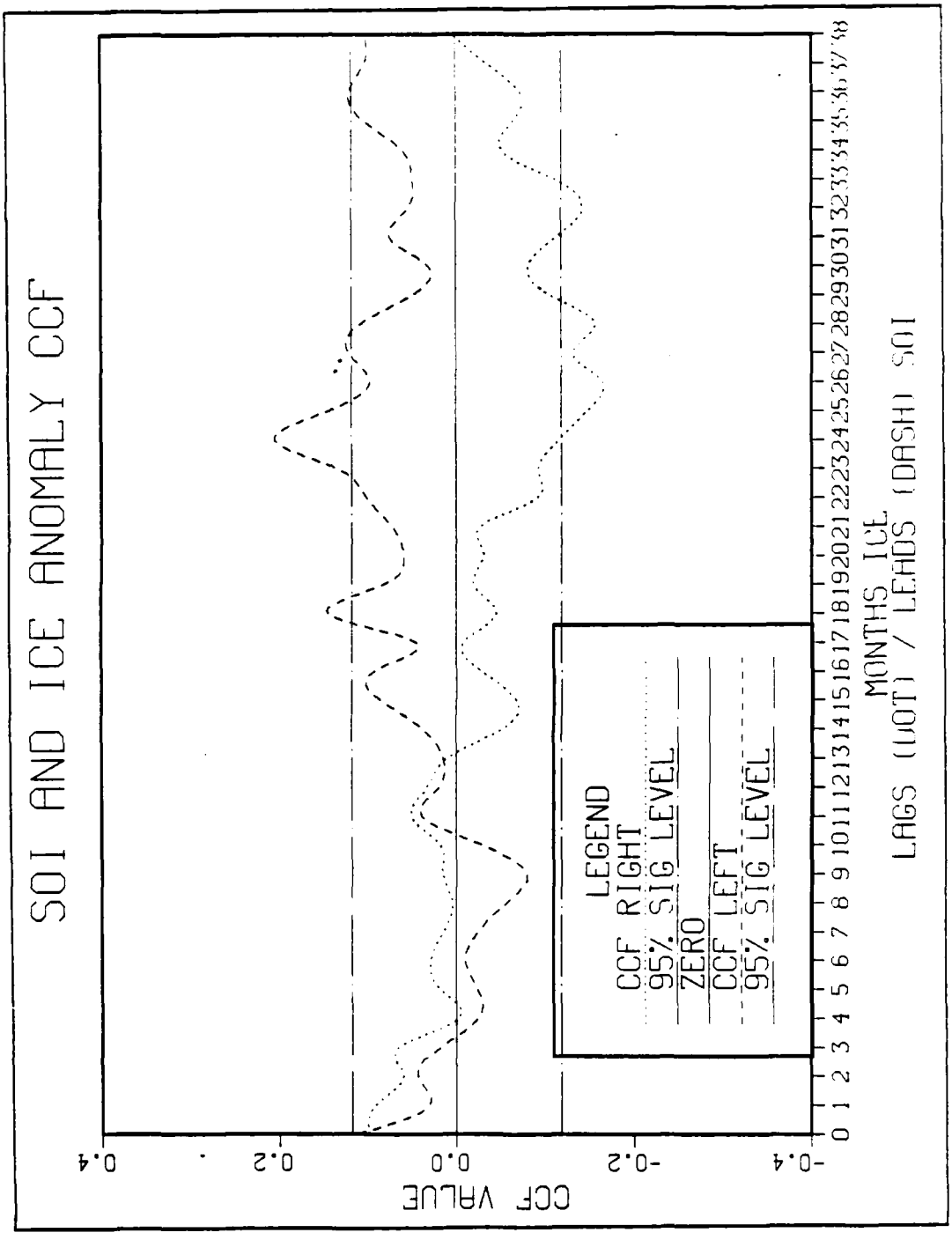

Figure 3.1 Cross-Correlation of SOI and Ice Anomalies by Month.

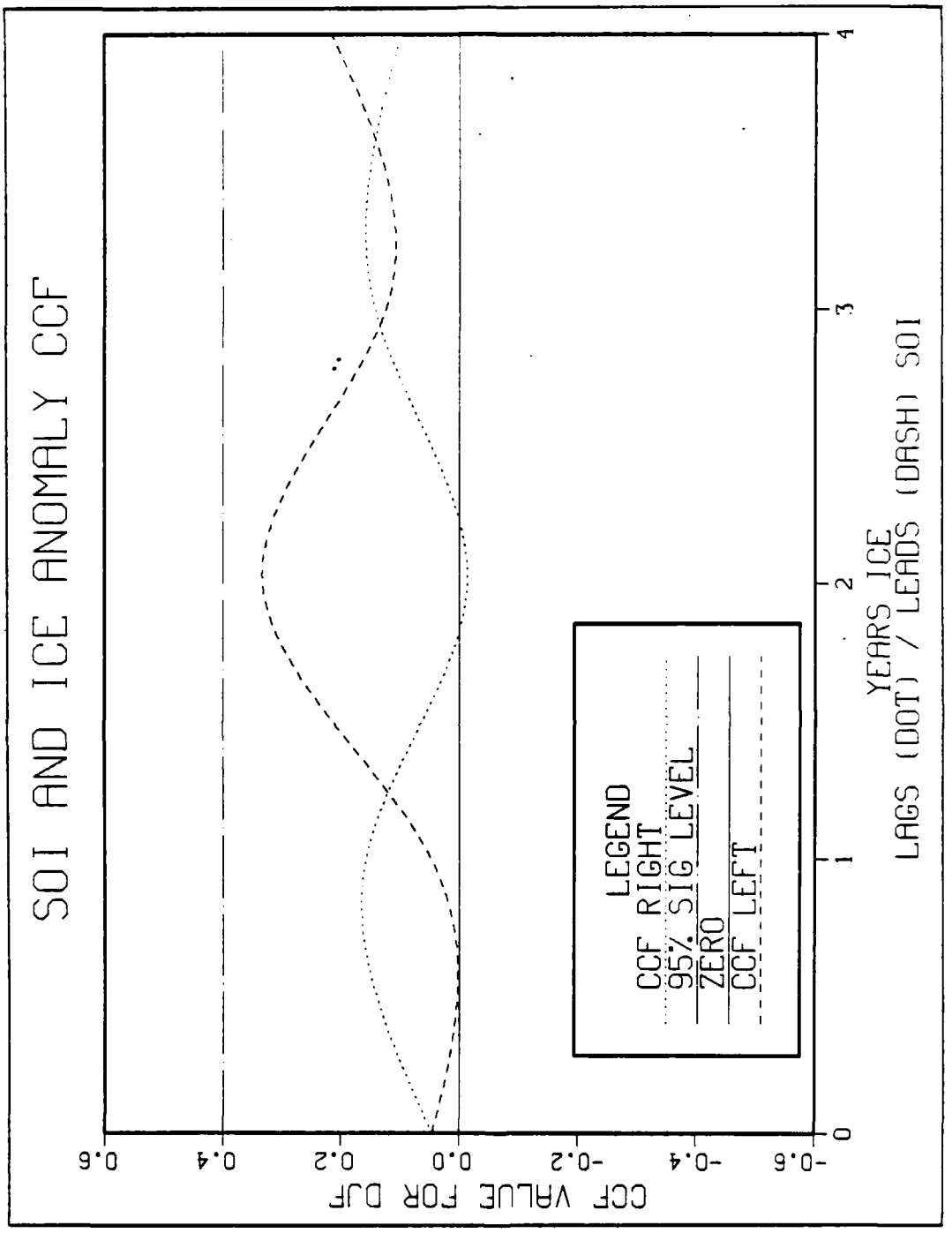

Figure 3.2 Cross-Correlation of SOI and Ice Anomalies for DJF.

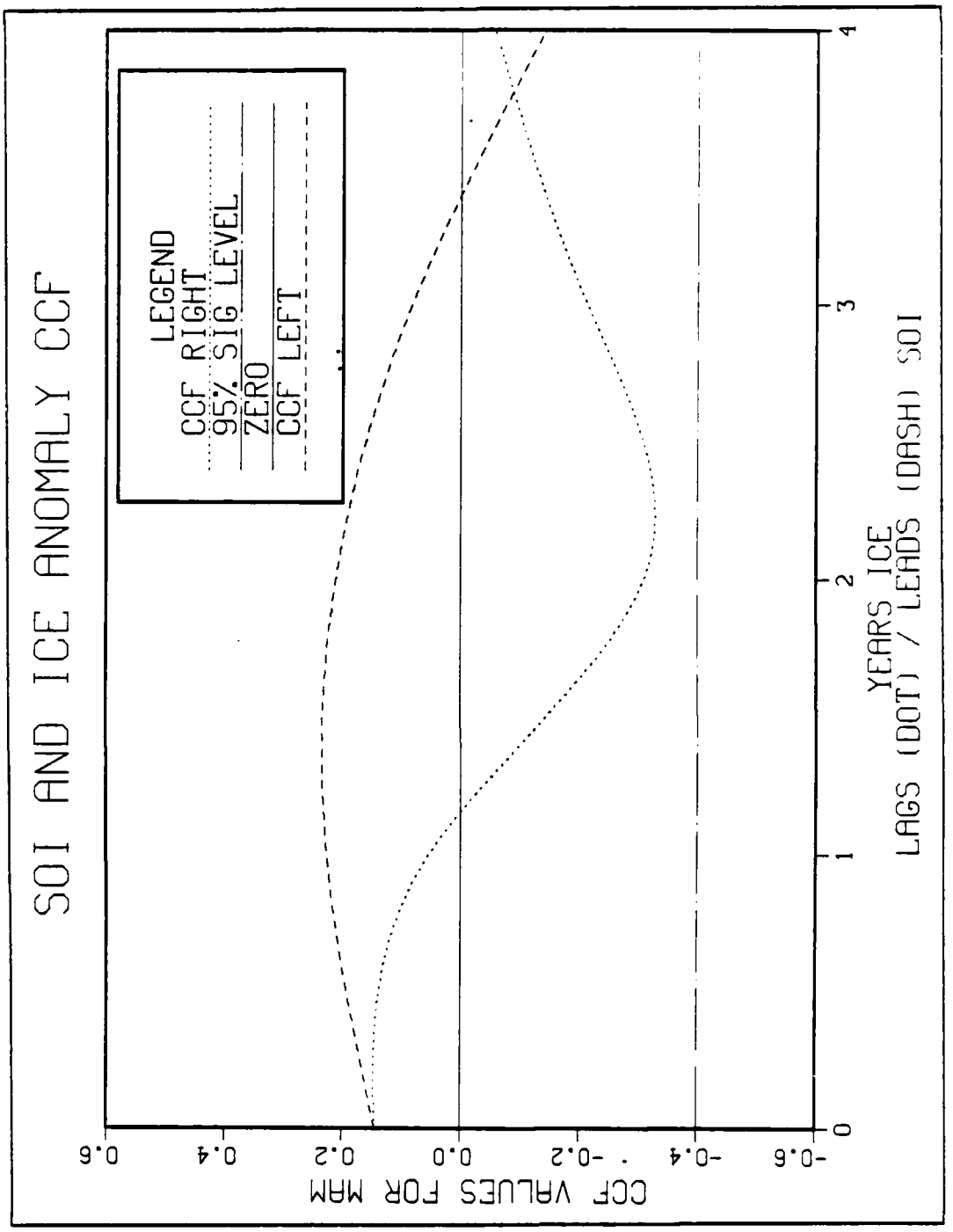

Figure 3.3 Cross-Correlation of SOI and Ice Anomalies for MAM.

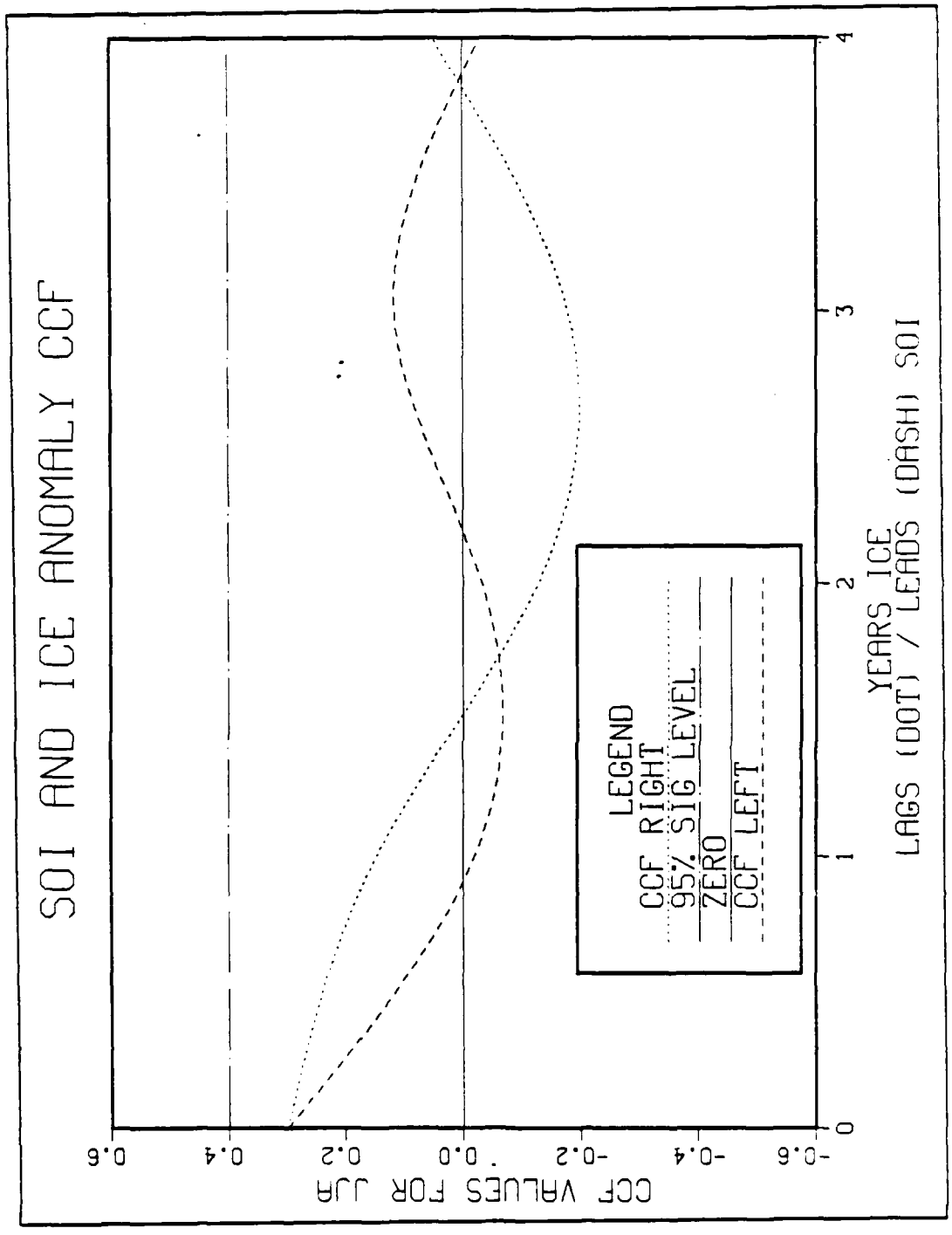

Figure 3.4 Cross-Correlation of SOI and Ice Anomalies for JJA.

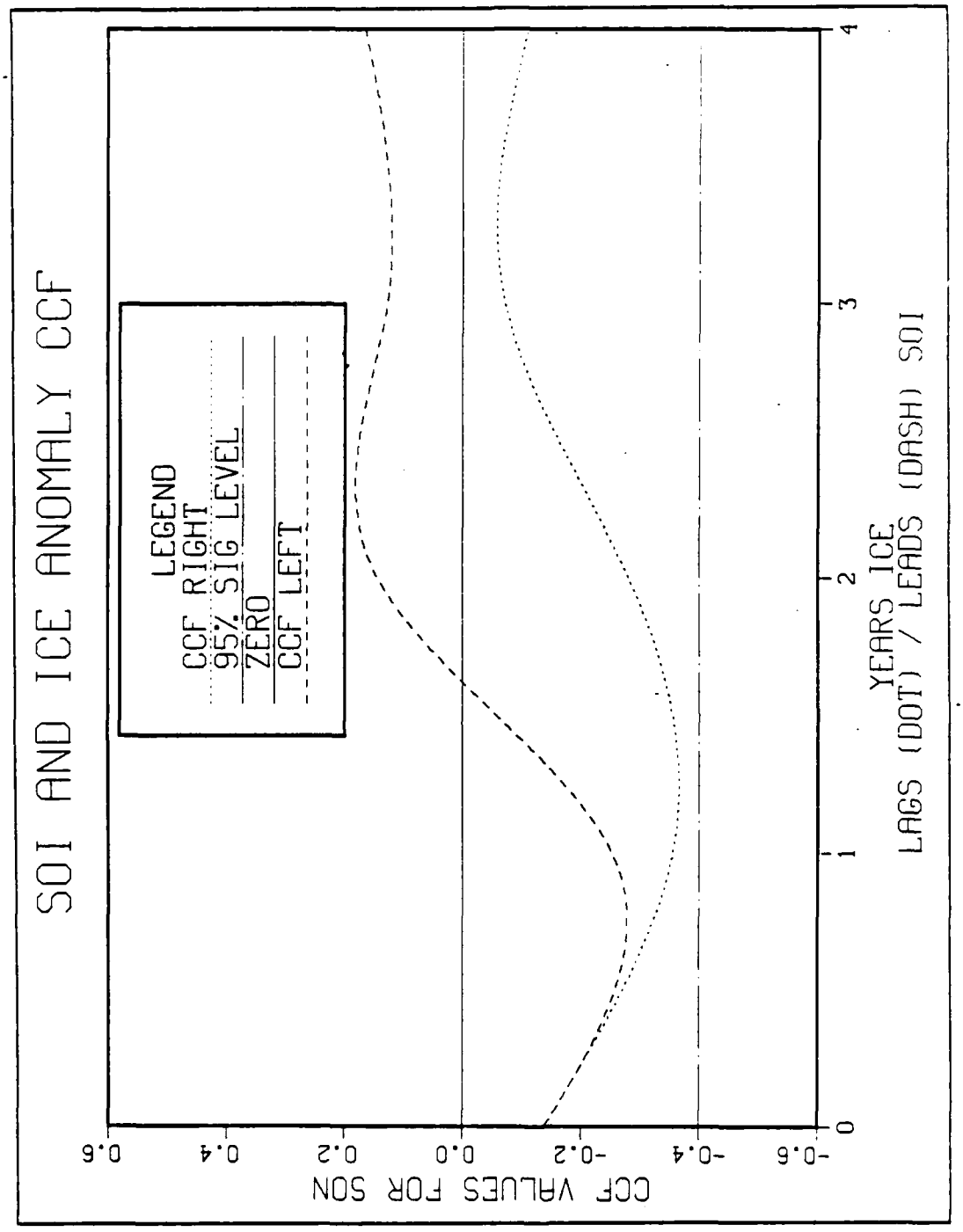

Figure 3.5 Cross-Correlation of SOI and Ice Anomalies for SON.

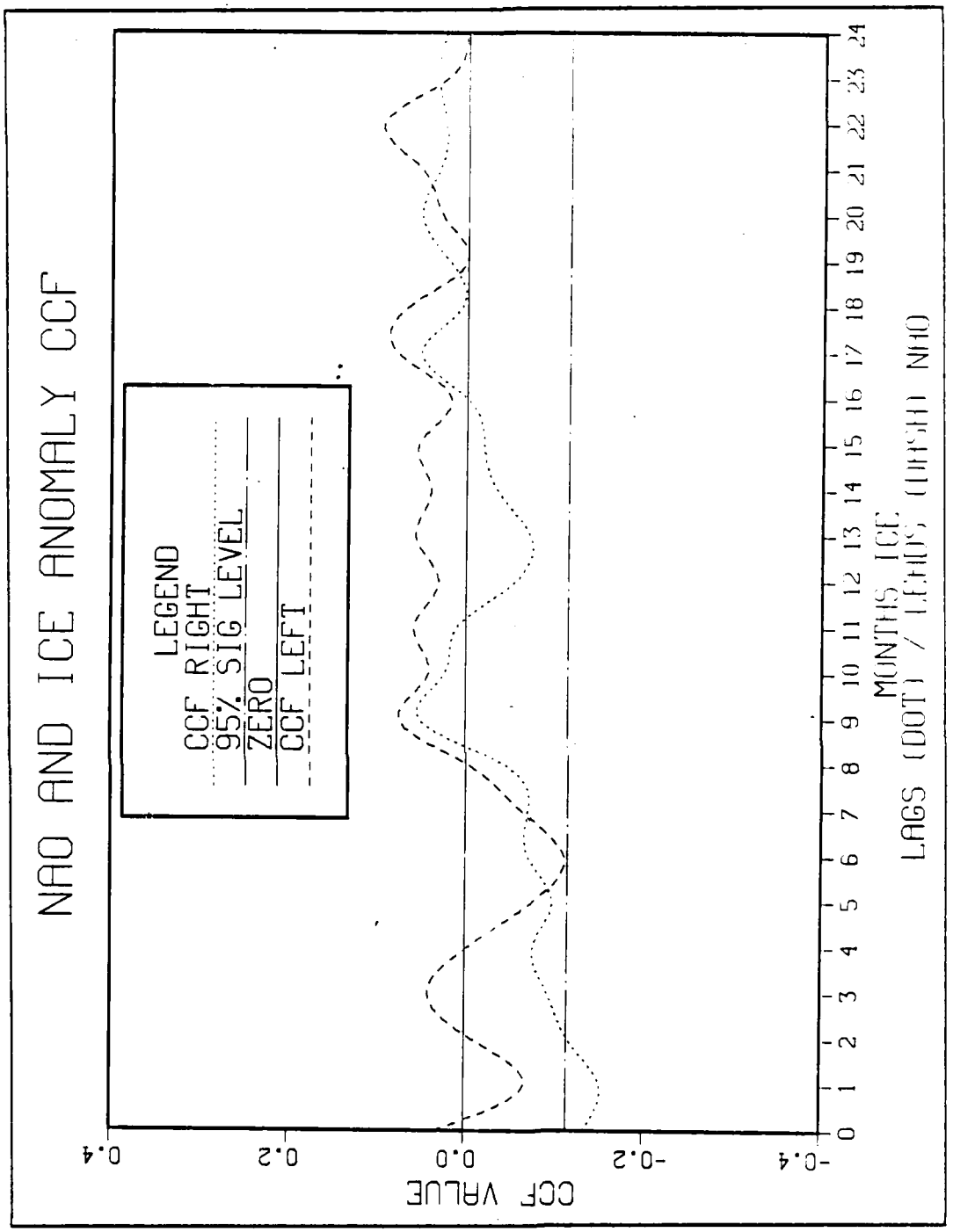

Figure 3.6 Cross-Correlation of NAO and Ice Anomalies by Month.

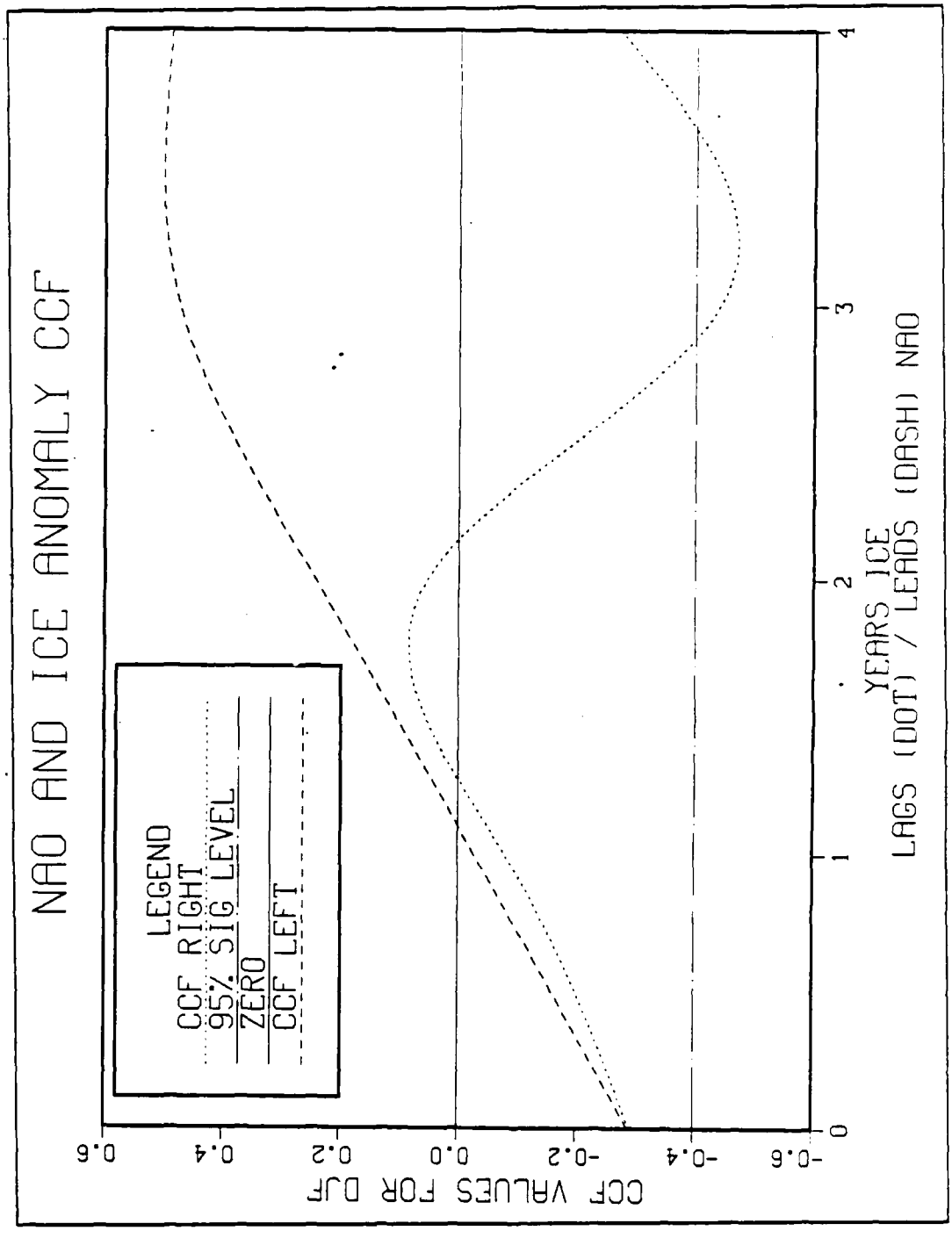

Figure 3.7 Cross-Correlation of NAO and Ice Anomalies for DJF.

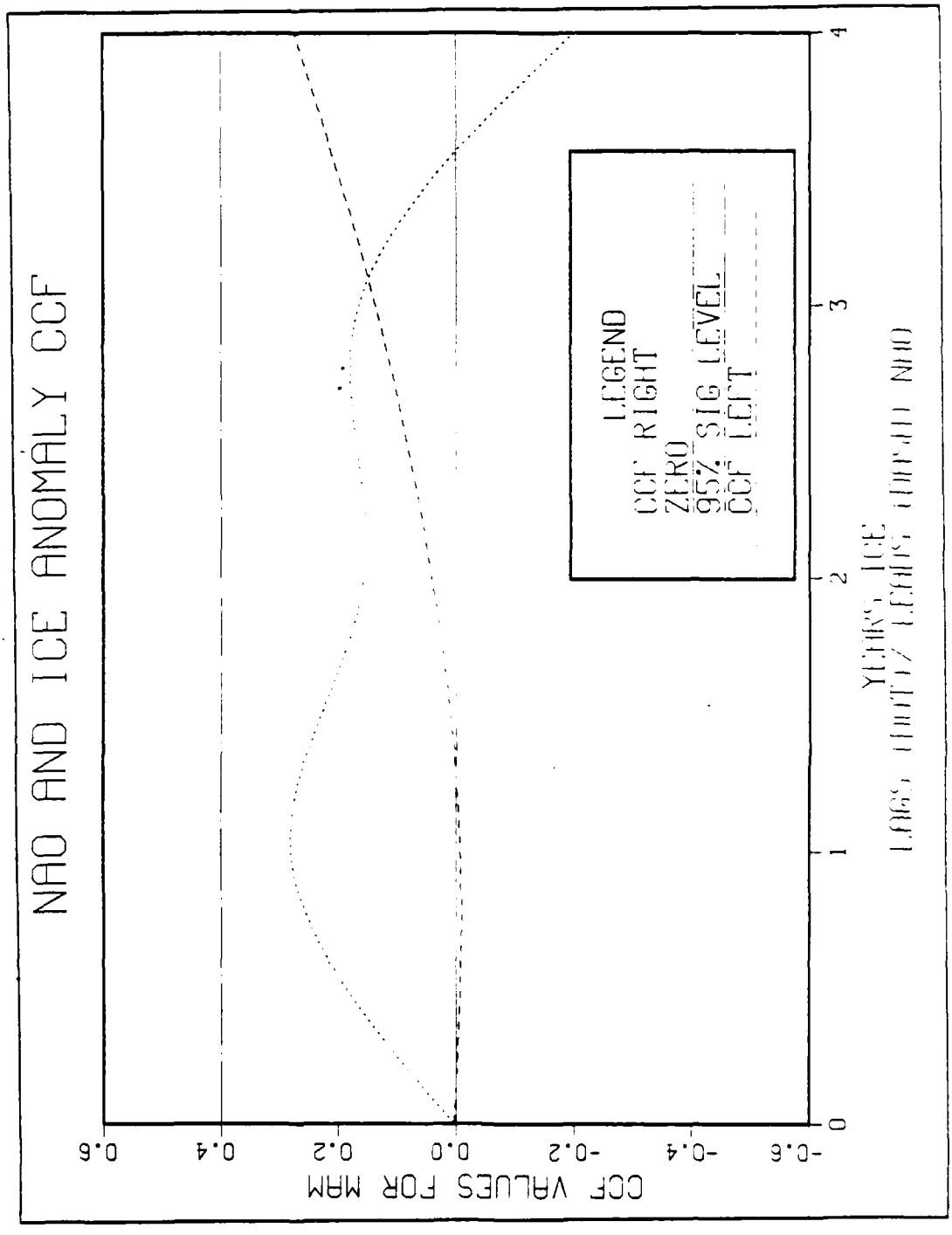

Figure 3.8 Cross-Correlation of NAO and Ice Anomalies for MAM.

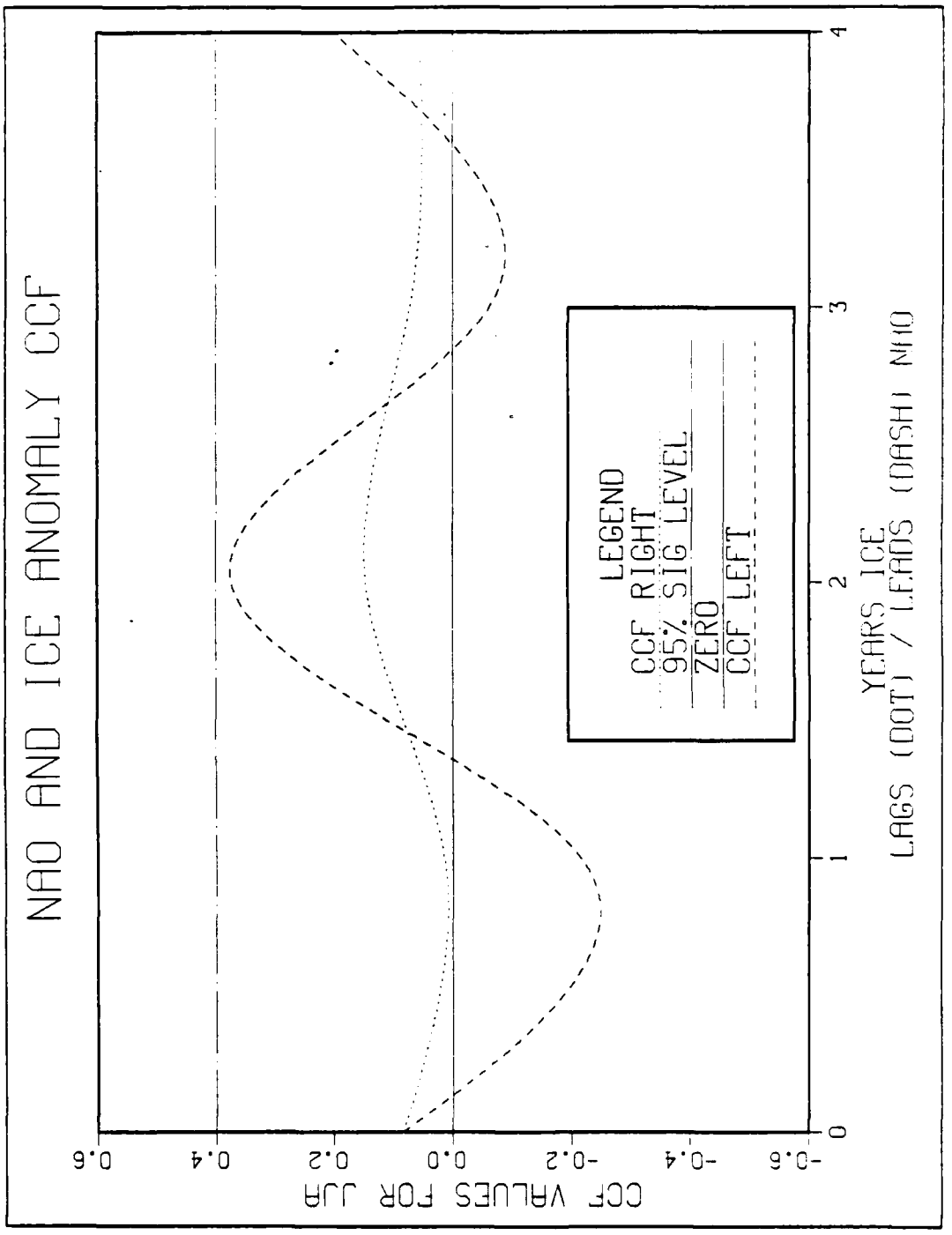

Figure 3.9 Cross-Correlation of NAO and Ice Anomalies for JJA.

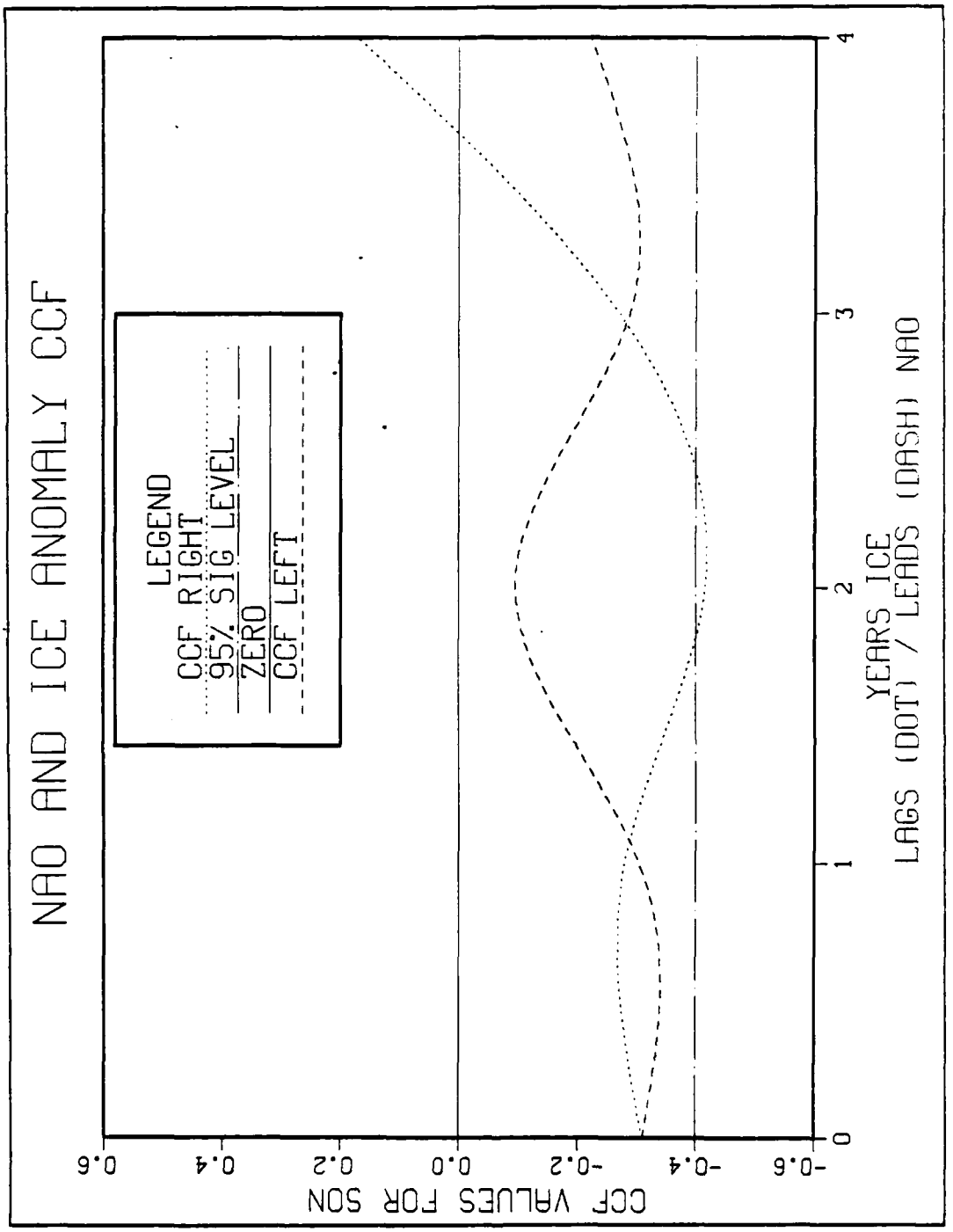

Figure 3.10 Cross-Correlation of NAO and Ice Anomalies for SON.

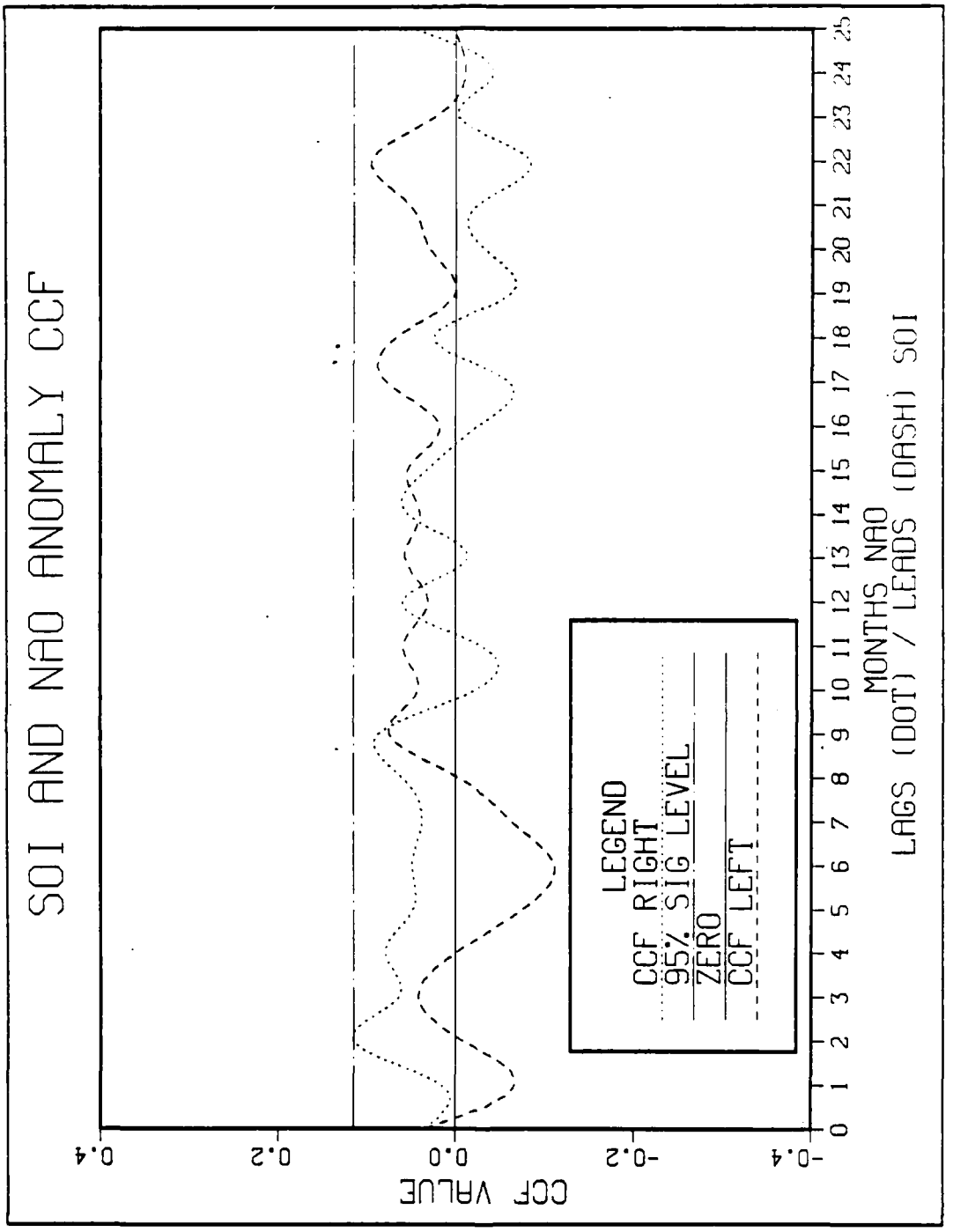

Figure 3.11 Cross-Correlation of SOI and NAO Anomalies by Month.

IV. SUMMARY, CONCLUSIONS, AND RECOMMENDATIONS

A. SUMMARY AND CONCLUSIONS

This study examined the hypothesis that the sea ice variability in the Greenland Sea is related to large scale weather patterns via atmospheric teleconnections. The weather patterns examined were the Southern Oscillation Index (SOI) and the North Atlantic Oscillation (NAO).

Time series plots of the monthly mean sea ice extent, SOI, and NAO were examined for the years 1953 to 1977 inclusive. Time series plots of the anomalies for the sea ice coverage, SOI, and NAO were constructed and examined. The 25-year time series for the sea ice anomaly shows increased ice coverage during the late 1960's. During the same period, Bering Sea ice showed a general decrease in sea ice extent, and Walsh and Sater (1981) discuss a marginal negative correlation between sea ice in the Bering and Greenland Sea. There appears to be a long period signal in the sea ice extent that is not possible to resolve with this data set. This long term signal in the sea ice extent may be related to the carbon dioxide in the atmosphere as suggested by Walsh (1983). The SOI time series anomalies clearly show the ENSO events for the 25-year period. Each ENSO event from 1953 to 1977 shows the SOI anomaly developing from a positive value into a negative one. The NAO time series signal is dominated by higher-frequency, shorter-period fluctuations than the SOI.

The anomalies for the sea ice extent were cross correlated with the anomalies of both the SOI and the NAO. The SOI anomaly is negatively correlated at time lags of 24 to 29 months where sea ice lags the SOI. This correlation

suggests that when the SOI anomaly is negative (as in ENSO years), the sea ice anomaly in the Greenland Sea is positive. Thus, there is more sea ice present at a time lag of 24 to 29 months. This particular correlation may result from the ice anomalies in the Bering Sea and the ice anomalies in the Greenland Sea being approximately 180 degrees out of phase. As shown by Niebauer (1986) the Bering Sea ice is positively correlated with the SOI anomalies from 0 to 2 years lag, where ice lags the SOI. This may suggest that the response time in sea ice extent for the Bering Sea and the Greenland Sea to the SOI may be of the order of two years.

The NAO anomaly is negatively correlated with the sea ice extent at 0 to 2 months lag where ice lags the atmosphere. This suggests that when the NAO is in a positive phase, there would be less ice in the Greenland Sea. This correlation probably comes from the circulation around the Icelandic Low. The atmospheric flow to the north of the low is nearly perpendicular to the flow of the East Greenland Current (EGC). This situation would tend to retard the advection of sea ice by the EGC due to packing the sea ice against the coast.

The anomaly for the areal extent of the sea ice was also cross-correlated by season with the SOI and NAO anomalies. Cross-correlations of sea ice with SOI or NAO anomalies do not reveal a significant relationship between the ice and these long term weather indexes.

The SOI anomaly was also cross-correlated with the NAO anomaly. The positive correlation was only marginally significant at a lag time of 2 months, with the NAO lagging the SOI. The NAO is a higher-frequency, shorter-period signal than the SOI and this may account for the marginal correlation.

A predominant source of error for this study is the sea ice data. The sea ice data were compiled from six different countries and is a conglomeration of visual observations and satellite observations. Sea ice type and thickness were not considered in this study.

B. RECOMMENDATIONS

Understanding the air-sea-ice interactions in the high latitude seas is important for the success of global models of ocean and atmospheric circulation. Examining some of the other atmospheric teleconnections such as the Pacific North American index and sea ice extent in the Greenland Sea could be useful. Examination of ocean variability, namely currents and eddies, and their effects on sea ice in the Greenland Sea would help resolve some of the local effects on sea ice extent. Other parameters that affect sea ice formation in the Greenland Sea, and that can be studied include sea surface temperature distribution, air temperature distribution, winds, and geopotential heights. Also, the study could be repeated for smaller areas of the Greenland Sea, identifying which specific locations (open ocean, coastal, etc.) are most sensitive to the atmospheric teleconnections.

LIST OF REFERENCES

Bjerknes, J., 1961: "El Nino" study based on analysis of ocean surface temperatures 1935-57. Inter-Amer. Trop. Tuna Comm. Bull., 12, 219-307.

Bjerknes, J., 1966: A possible response of the atmospheric Hadley circulation to equatorial anomalies of ocean temperature. Tellus, 18, 820-829.

Bjerknes, J., 1969: Atmospheric teleconnections from the equatorial Pacific. Mon. Wea. Rev., 97, 163-172.

Coachman, L.K., and K. Aagaard, 1974: Physical oceanography of arctic and sub-arctic seas, in Marine Geology and Oceanography of the Arctic Seas, Y. Herman, editor, Springer-Verlag, New York, 1-81.

Horel, J.D. and J.M. Wallace, 1981: Planetary-scale atmospheric phenomena associated with the Southern Oscillation. Mon. Wea. Rev., 109, 813-829.

Ketchum R.D., Jr., and W.I. Wittmann, 1972: Recent remote sensing studies of the East Greenland pack ice, in Sea Ice, T. Karlsson, editor, National Research Council, Reykjavik, 213-224.

Kutzbach, J.E., 1970: Large-scale features of monthly mean Northern Hemisphere anomaly maps of sea-level pressure. Mon. Wea. Rev., 98, 708-716.

Niebauer, H.J., 1984: On the effect of El Nino in Alaskan waters. Bull. Am. Meteorol. Soc., 65, 2733-2742.

Niebauer, H.J., 1986: El Nino-Southern Oscillation teleconnections with the subarctic Bering Sea. Submitted to J. Geophys. Res.

Pickard, G.L., and W.J. Emery, 1982: Descriptive Physical Oceanography, fourth ed., Pergamon Press, 249 pp.

Quinn, W.H., D.O. Zoph, K.S. Short, and R.T.W. Kuo Yang, 1978: Historical trend and statistics of the Southern Oscillation, El Nino, and Indonesian droughts. Fish. Bull., 76, 663-678.

Rasmusson, E.M., and T.H. Carpenter, 1982: Variations in tropical sea surface temperature and surface wind fields associated with the Southern Oscillation/El Nino. Mon. Wea. Rev., 110, 354-384.

Sater, J.E., A.G. Ronhovde, and L.C. Van Allen, 1971: Arctic Arctic Environment and Resources, The Arctic Institute of North America, 309 pp.

Smirnov, V.I., 1980: Opposition in ice redistribution in the waters of the foreign Arctic, Meteorol. Gidrol., 108, 73-77.

Trenberth, K.E., 1984: Signal versus noise in the Southern Oscillation. Mon. Wea. Rev., 112, 326-332.

Urick, R.J., 1983: Principles of Underwater Sound, Third ed., McGraw-Hill Book Company, 423 pp.

van Loon, H., and J.C. Rogers, 1978: The seesaw in winter temperatures between Greenland and Northern Europe. part 1: general description. Mon. Wea. Rev., 106, 296-310.

Walker, G.T., and E.W. Bliss, 1932: World weather V. Mem. Roy. Meteor. Soc., 4, 53-84.

Wallace, J.M., and D.S. Gutzler, 1981: Teleconnections in the geopotential height field during the Northern Hemisphere winter. Mon. Wea. Rev., 109, 784-812.

Walsh, J.E., 1983: The role of sea ice in climatic variability: theories and evidence. Atmosphere-Ocean, 21, 229-242.

Walsh, J.E., and C.M. Johnson, 1979: An analysis of Arctic Sea ice fluctuations, 1953-1977. J. Phys. Oceanogr., 9, 580-591.

Walsh, J.E., and J.E. Sater, 1981: Monthly and seasonal variability in the ocean-ice-atmosphere systems of the North Pacific and the North Atlantic. J. Geophys. Res., 86, 7425-7445.

Weeks, W.F., 1978: Arctic Sea Ice, Part 1, in Glaciological Data, World Data Center A For Glaciology Report GD-2, 20 pp.

Wyrtki, K., 1975: El Nino - the dynamic response of the equatorial Pacific Ocean to atmospheric forcing. J. Phys. Oceanogr., 5, 572-584.

Wyrtki, K., 1982: The Southern Oscillation, ocean-atmosphere interaction and El Nino. Mar. Technol. Soc. J., 16, 3-10.

INITIAL DISTRIBUTION LIST

		No. Copies
1.	Defense Technical Information Center Cameron Station Alexandria, VA 22304-6145	2
2.	Library, Code 0142 Naval Postgraduate School Monterey, CA 93943-5000	2
3.	Chairman (Code 68Mr) Department of Oceanography Naval Postgraduate School Monterey, CA 93943	1
4.	Chairman (Code 63Rd) Department of Meteorology Naval Postgraduate School Monterey, CA 93943	1
5.	Professor Roland W. Garwood (Code 68Gd) Department of Oceanography Naval Postgraduate School Monterey, CA 93943	2
6.	Professor H.J. Niebauer Institute of Marine Sciences University of Alaska - Fairbanks Fairbanks, AK 99701	2
7.	Miss Arlene Bird (Code 68) Department of Oceanography Naval Postgraduate School Monterey, CA 93943	1
8.	Director Naval Oceanography Division Naval Observatory 34th and Massachusetts Avenue NW Washington, D.C. 20390	1
9.	Commander Naval Oceanography Command NSTL Station Bay St. Louis, MS 39522	1
10.	Commanding Officer Naval Oceanographic Office NSTL Station Bay St. Louis, MS 39522	1
11.	Commanding Officer Fleet Numerical Oceanography Center Monterey, CA 93943	1
12.	Commanding Officer Naval Ocean Research and Development Activity NSTL Station Bay St. Louis, MS 39522	1
13.	Commanding Officer Naval Environmental Prediction Research Facility	1

Monterey, CA 93940

14. Chairman, Oceanography Department 1
U.S. Naval Academy
Annapolis, MD 21402

15. Chief of Naval Research 1
800 N. Quincy Street
Arlington, VA 22217

16. Office of Naval Research (Code 420) 1
Naval Ocean Research and Development Activity
800 N. Quincy Street
Arlington, VA 22217

17. LT. Ward Wilson 3
1611 Kirkwood rd
Baltimore, MD 21207

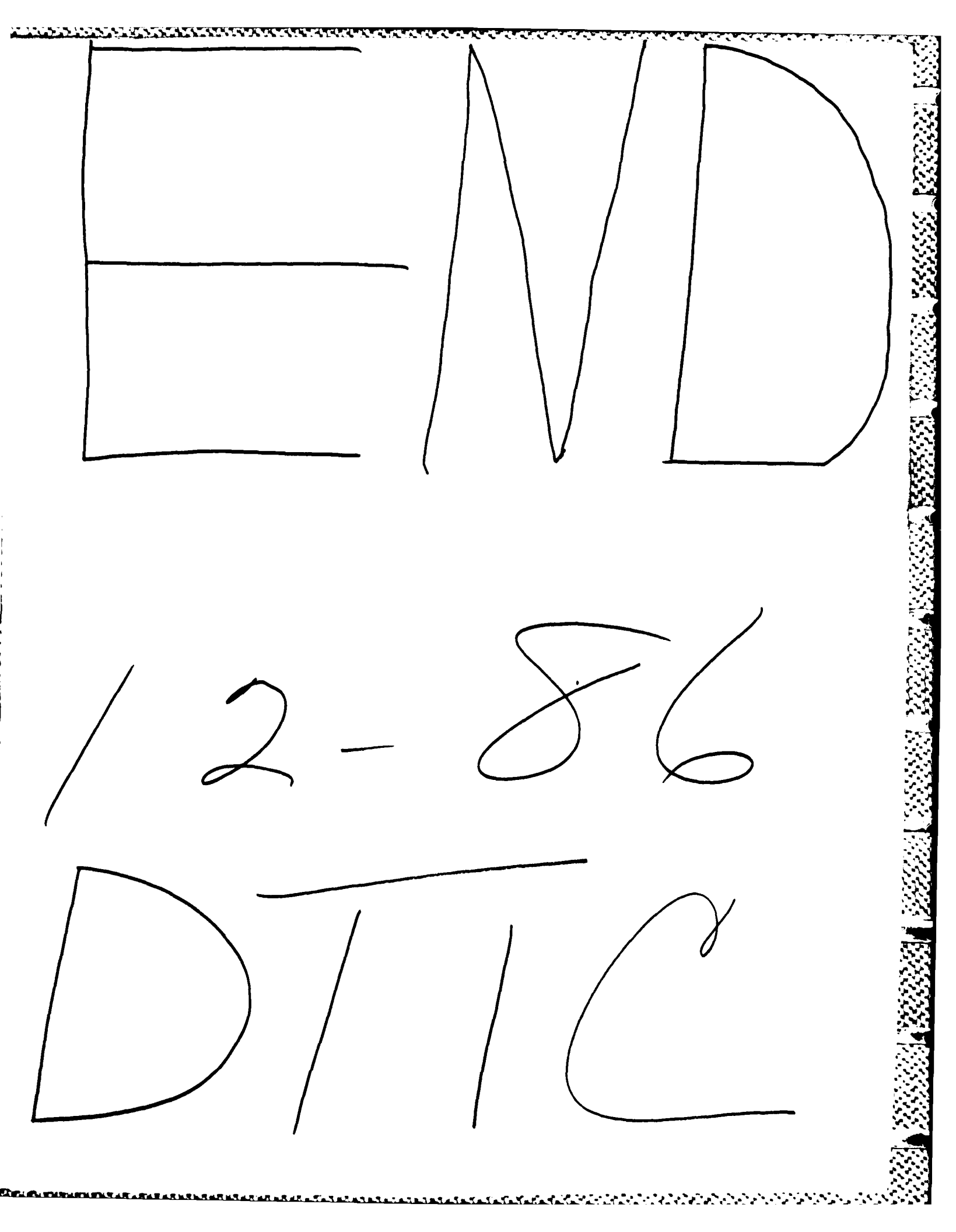
FMD
12-86
DTIC